

Quasi-degenerate heavy neutral leptons in the left-right symmetric model

Mikulenko, O.

Citation

Mikulenko, O. (2025). Quasi-degenerate heavy neutral leptons in the left-right symmetric model. *Jhep Reports*, 2025. doi:10.1007/JHEP06(2025)023

Version: Publisher's Version

License: <u>Creative Commons CC BY 4.0 license</u>

Downloaded from: <u>https://hdl.handle.net/1887/4281853</u>

Note: To cite this publication please use the final published version (if applicable).



RECEIVED: September 17, 2024 REVISED: March 31, 2025 ACCEPTED: May 6, 2025 PUBLISHED: June 4, 2025

Quasi-degenerate heavy neutral leptons in the left-right symmetric model

Oleksii Mikulenko

Instituut-Lorentz, Leiden University, Niels Bohrweg 2, 2333 CA Leiden, The Netherlands

E-mail: mikulenko@lorentz.leidenuniv.nl

ABSTRACT: We discuss the phenomenology of a pair of degenerate GeV-scale Heavy Neutral Leptons within the Left-Right Symmetric Model (LRSM) framework, with the third fermion serving as a dark matter candidate. We highlight the potential of the recently approved SHiP experiment to test the existence of a light dark matter species, and signatures of lepton number violation as a possible experimental probe of the model in various experiments. Our findings include concrete predictions for the effective right-handed couplings $(V_e^R)^2$: $(V_\mu^R)^2:(V_\tau^R)^2=0.16:0.47:0.38$ (normal neutrino hierarchy), 0.489:0.22:0.30 (inverted hierarchy) of the degenerate HNL pair, and $(V_e^R)^2:(V_\mu^R)^2:(V_\tau^R)^2=0.68:0.07:0.24$ (normal), 0.02:0.57:0.41 for the dark matter candidate.

KEYWORDS: Sterile or Heavy Neutrinos, Left-Right Models, Baryon/Lepton Number Violation, Dark Matter at Colliders

ARXIV EPRINT: 2406.13850

Co	ontents	
1	Introduction	1
2	Phenomenology of HNLs below the electroweak scale	3
3	Flavor structure from the seesaw relation	6
	3.1 LRSM Lagrangian	6
	3.2 The approximate symmetry limit	8
4	Experimental probes	12
	4.1 Sensitivity of FCC-ee in the Z -pole mode	12
	4.2 (De)coherence of the quasi-degenerate pair	15
	4.3 Dark matter at SHiP	20
5	Conclusions	23
\mathbf{A}	Decay $N_I o N_J l_lpha l_eta$	24
В	Parametrization of the seesaw relation	25

1 Introduction

The Standard Model (SM) has achieved remarkable success in describing physics at energies up to the electroweak scale, both in collider experiments and in the universe. Several phenomena, however, still lack an explanation in the SM: the existence of nonluminous, nonbaryonic dark matter that permeates the universe; masses of neutrinos, manifesting in the oscillations between different flavors; and the striking asymmetry between matter and antimatter in our universe. A minimalistic and natural scenario capable of handling all the aforementioned beyond the SM (BSM) problems is the introduction of right-handed counterparts of the SM neutrinos, i.e. sterile neutrinos [1-4]. As the name indicates, these new particles are not charged under any of the SM gauge groups, may have Majorana mass, and are an example of more general Heavy Neutral Leptons (HNL), see [5, 6] for a review. Despite being sterile, the new particles possess a feeble weak-like interaction as a consequence of their mixing with active neutrinos. The interaction is suppressed by the small mixing angle $U \ll 1$ and creates the opportunity to search for these elusive particles at future accelerator experiments, such as SHiP [7, 8], DUNE [9-11], LHC-based experiments [12-19], and future colliders [20-26]. In addition to this, HNLs can be constrained with astrophysics and cosmology [27–39] and indirect searches such as electroweak precision measurements [40-42], neutrino double-beta decay [43-45], and charge lepton number violation [46-48].

The future experiments envisioned can observe HNLs with couplings that are orders of magnitude beyond the current limits. Consequently, there is a potential for abundant signal yield, which would facilitate scrutinizing the properties of the newly seen particles [49, 50].

A natural question then arises: what is the landscape of models that could, in principle, lead to such an observed signal, and how can we differentiate between these models? This question is the main motivation of the presented work.

The neutrino Minimal Standard Model (ν MSM) [51, 52] introduces one keV-scale sterile neutrino N_1 and two heavier HNLs N_2 , N_3 with masses at or above the GeV scale. For the naming convention, we will denote the heavy species that can be probed by direct searches as HNLs (N_2, N_3) in this case). The sterile neutrino N_1 serves as a warm dark matter candidate [53, 54] and has a somewhat narrow range of possible masses around the keV scale, bounded from below by the Tremaine-Gunn bound [55, 56] and from above by the X-ray emission constraints from DM-dominated objects [57]. The two HNLs lead to two massive neutrino states via the so-called type-I seesaw mechanism, leaving the lightest active neutrino effectively massless. The naive scale of the HNL mixing angles is then defined by the seesaw limit $U_{\text{seesaw}}^2 = \sqrt{\Delta m_{\text{atm.}}^2}/m_N$, with $\Delta m_{\text{atm.}}^2 = (50 \,\text{meV})^2$ being the mass scale of the active neutrinos. This scale is too small to be reached by the mentioned future experiments. An attractive theoretical scenario is to consider the HNL pair in the quasi-Dirac limit [58], which alleviates some problems. First, an approximate lepton symmetry translates into a cancellation between the two seesaw contributions: the mixing angles of HNLs may be large, within the reach of the near-future experiments, without spoiling active neutrino masses. Second, there is limited freedom in the relations between the coupling constants to different lepton flavors, making the model less generic and more easily verifiable. Finally, oscillations between the two GeV degenerate HNLs may enhance the efficiency of leptogenesis [59–63], a possible mechanism for the generation of the baryon asymmetry in the universe [64, 65] which is otherwise viable only for HNL masses (much) above the electroweak scale. Ultimately, the model deals with the three BSM phenomena and is a very attractive target for searches.

Beyond the minimal model, HNLs can possess additional interactions, which may affect searches for such particles [66–71]. One model that naturally leads to such nonminimal interactions is the Left-Right Symmetric Model (LRSM) [2, 3, 72], attempting to restore the symmetry between the left and right particles. The model extends the SM with a new SU(2)_R gauge symmetry and equips HNLs, the right-handed neutrino siblings in this case, with interactions through the right-handed charged current. The new symmetry is spontaneously broken at a scale higher than the electroweak scale, and the processes with the right-handed analog W_R of the W-boson are suppressed by the large mass of the mediator $m_{W_R} \gg m_W$. The constraints on the scale of new physics come from direct searches [73–77], meson precision measurements [78, 79], and neutrinoless double beta decay [80–82]. Current limits on the mass of the new boson generally lie around or below 5 TeV.

In this work, we embed the ν MSM-motivated case of one sterile neutrino and two HNLs in the approximate symmetry limit into the minimal Left-Right Symmetric Model. The symmetry no longer conserves lepton number, explicitly broken by the new gauge interactions. We study the flavor structure of the HNL couplings and analyze the additional signatures arising from the new interactions, based solely on the seesaw relation between the couplings and the active neutrino masses. Specifically, we found an analytic form of the leptonic analog

¹This neglects the contribution of the dark matter N_1 , whose effect is tiny due to the constraints on the particle's lifetime.

 V^R of the CKM matrix in the approximate symmetry limit. For some experimental setups, the HNL pair can be described as a single particle with an effective coupling, uniquely fixed by the experimentally measured properties of active neutrinos.

It must be stressed that the proposed embedding has a few problems. From the phenomenological perspective, we treat the ν MSM as a limit of the LRSM, in which the energy scale of new gauge bosons is too high to affect experimental searches. The DM candidate N_1 remains cosmologically stable if it is lighter than the electron, since the decay through right-handed current is kinematically forbidden. However, the inclusion of gauge interactions with the new scale in the 10 TeV – 100 TeV range (within the reach of collider experiments) introduces an additional means of thermalization for particles in the early universe. This poses severe obstacles to the model's capability to account for both baryon asymmetry [83–86] and dark matter [87]. Thus, some additional mechanisms are needed for the model to be viable. The thermal overproduction of dark matter may be avoided with a period of early matter domination by some heavy particles, diluting the abundance of hot relics [88, 89], although the realization of such a scenario within the experimentally interesting region is challenging [90, 91].

The structure of the paper is as follows. Section 2 describes the phenomenology of HNLs with combined left and right-current interactions. In section 3, we constrain the flavor structure of the left and right coupling constants from the LRSM Lagrangian. Section 4 discusses various interesting experimental signatures of the considered model, specifically the lepton number violation signatures and dark matter search at the SHiP experiment. We conclude in section 5.

2 Phenomenology of HNLs below the electroweak scale

In this section, we summarize the phenomenology of a unified left-plus-right interaction of HNLs that will be relevant to us. Without going into details, we assume that the gauge symmetry contains two subgroups $SU_L(2)$ and $SU_R(2)$ that are coupled respectively to left- and right-handed fermions, and which are spontaneously broken at different scales. The scale of symmetry breaking of $SU_R(2)$ is higher, making the associated gauge bosons much heavier than the SM W, Z-bosons. Right-handed HNLs are connected to the light SM fermions via the charged boson W_R and through the Yukawa couplings to neutrinos (mixing). These interactions are described by the following terms in the Lagrangian that contain left-handed (LH) current coupled with the SM gauge bosons W, Z and right-handed (RH) current coupled to a new W_R boson:

$$\mathcal{L}_{L} \supset \frac{g}{\sqrt{2}} \bar{l}_{\alpha} N_{I}^{c} W + \frac{g}{2 \cos \theta_{W}} \bar{\nu}_{\alpha} N_{I}^{c} Z + \text{h.c.}$$

$$\mathcal{L}_{R} \supset \frac{g}{\sqrt{2}} \bar{l}_{\alpha} N_{I} W_{R} + \text{h.c.}$$

where N_I is a right-handed Weyl spinor representing an HNL, and $\alpha = e, \mu, \tau$ are leptonic flavors. The neutral current νN emerges only through mixing between left and right fermions and is absent in \mathcal{L}_R . In principle, left and right bosons can mix with each other: thus, W may mediate the RH interactions as well. We do not consider such interactions since these

depend on the UV completion of the model and are likely to be suppressed, see section 3.2. The mixing between Z and its heavier counterpart Z_R is relevant in the Z-pole experiments and is considered separately in section 4.1. The interactions mediated by the scalar sector of the model are not considered here: we expect them to be subdominant because of an additional suppression from the Yukawa couplings of particles in the considered GeV-scale. A review of all interactions in LRSM can be found in [92].

For HNLs below the electroweak scale, the interactions unify into a generalized Fermi interaction with both left and right currents:

containing some phenomenological couplings, with G_F being the Fermi constant and J_Z being the SM neutral current. Both types of interactions are suppressed by small parameters² $\theta_{L,R} \ll 1$. To separate the suppression scale and the flavor structure, it is useful to reparametrize them in the form

$$\theta^L_{\alpha I} \equiv U^L_I V^L_{\alpha I}, \qquad \theta^R_{\alpha I} \equiv U^R_I V^R_{\alpha I}, \qquad \sum_{\alpha} |V^{R/L}_{\alpha I}|^2 = 1.$$

The Lagrangian (2.1) may be viewed as an effective theory with a set of arbitrary couplings. For some experimental probes, the constraints on the θ_L can be recast into the equivalent bounds for θ_R . For example, this can be applied to the $0\nu\beta\beta$ bounds [93]; one has to be careful, however, with the possible interference effects [81]. An example of a study that includes both types of interactions can be found in [94]. The Left-Right symmetric model imposes the following constraints. First, there are 3 HNL species, and the right-handed suppression scale³ $U_I^R = m_W^2/m_{W_R}^2$ is equal for all species. Second, the unspecified couplings $\tilde{V}_{J\beta}^R$ that appear in two-HNL interaction terms must be equal to $(V_{\beta J}^R)^*$. Finally, the right-handed CKM matrix $V^{R,\text{CKM}}$ is approximately equal to the standard CKM matrix, up to the corrections that are bounded from above by $2m_b/m_t \approx 0.05$ [95]. In this work, we assume that these two CKM matrices are equal.

The phenomenology of HNLs with only mixing interactions, $U^R = 0$, has been reviewed in [96]. The main qualitative difference that arises from the inclusion of right-handed interactions is the appearance of the interaction between different HNL species. In the minimal case, such interactions are suppressed by the small left-handed couplings twice, once per each HNL involved. The additional interaction opens up an opportunity to observe HNLs that would otherwise be inaccessible.

Below, we list the relevant production and decay channels for the model.

²We use the upper and lower-index notation $\theta^L = \theta_L$, $V^R = V_R$, etc., interchangeably.

³Or, generally, $U_R = g_R m_W^2 / g_L m_{W_R}^2$, if one does not impose the equality of the left and right gauge couplings $g_L \neq g_R$.

Production. For beam-dump experiments, the main HNL production channel is the decay of copiously produced mesons. Since strong interactions respect parity, the meson form-factors remain the same regardless of whether the decay happens through the left or the right quark current. The branching ratio for decay of a meson X has the following scaling:

$$Br(X \to Y l_{\alpha} N_I) = (|\theta_{\alpha I}^L|^2 + |\theta_{\alpha I}^R|^2) Br_{norm.}(X \to Y l_{\alpha} N_{\alpha})$$

where (norm.) with N_{α} stands for a quantity, normalized to $\theta_{\alpha I} = 1$ and the other couplings with $\beta \neq \alpha$ set to zero. These can be found in [96].

At LHC and future high-energy colliders [14, 16, 17, 21], decays of W, Z (and H) become relevant. They can happen through the left current

$$Br(W, Z, H \to \nu_{\alpha} N_I) = |\theta_{\alpha I}^L|^2 Br_{norm.}(W, Z, H \to \nu_{\alpha} N_{\alpha})$$

and, in principle, through right-handed current as a result of mixing between W, Z and their right-handed counterparts. The branching ratios cannot be parametrized by the couplings θ^R ; one has to specify the UV-completion of the model.

For searches at even higher energies, with HNL mass above the electroweak scale, direct production starts to play a role, such as in the famous Keung-Senjanovic process [97].

Decays. The HNL decay modes are shown in figure 1.

(a) Hadronic decays through the charged current are mediated by both interactions and have equal scaling:

$$\Gamma(N_I \to l_{\alpha}h^+) = (|\theta_{\alpha I}^L|^2 + |\theta_{\alpha I}^R|^2)\Gamma_{\text{norm.}}(N_{\alpha} \to l_{\alpha}h^+),$$

under our assumption of the equality of left and right-handed CKM matrices. These decays result in a fully detectable state of a charged lepton and hadrons.

(b) Decays into neutral hadrons and neutrino are mediated only by the left-handed interaction

$$\Gamma(N_I \to \nu_{\alpha} h^0) = |\theta_{\alpha I}^L|^2 \Gamma_{\text{norm.}}(N_{\alpha} \to \nu_{\alpha} h^0)$$

- (c) Purely leptonic decays $\Gamma(N_I \to \nu l \bar{l} \text{ or } 3\nu) \propto |\theta^L|^2$ are mediated only by the left-handed interaction.
- (d) Finally, the additional channel of decay into a lighter HNLs $N_I \to N_J l_\alpha \bar{l}_\beta$ is suppressed only once despite involving two HNL species. There are two diagrams for this process (figure 2) that, in general, interfere with each other. However, if the lighter species is substantially lighter than the decaying HNL, the two diagrams decouple and correspond to the emission of N_J with specific helicity: positive (negative) helicity when N_J acts as a particle (antiparticle). In this limit, the total decay width reads

$$\Gamma(N_I \to N_J l_\alpha \bar{l}_\beta) = U_R^2 \left(|V_{\alpha I}^R|^2 |V_{\beta J}^R|^2 + |V_{\beta I}^R|^2 |V_{\alpha J}^R|^2 \right) \Gamma_{\text{norm.}} (N_\alpha \xrightarrow{W} l_\alpha \nu_\beta \bar{l}_\beta)$$

The decay is mediated only by the W_R boson. The full expression for the decay width with nonvanishing m_{N_J} is given in appendix A.

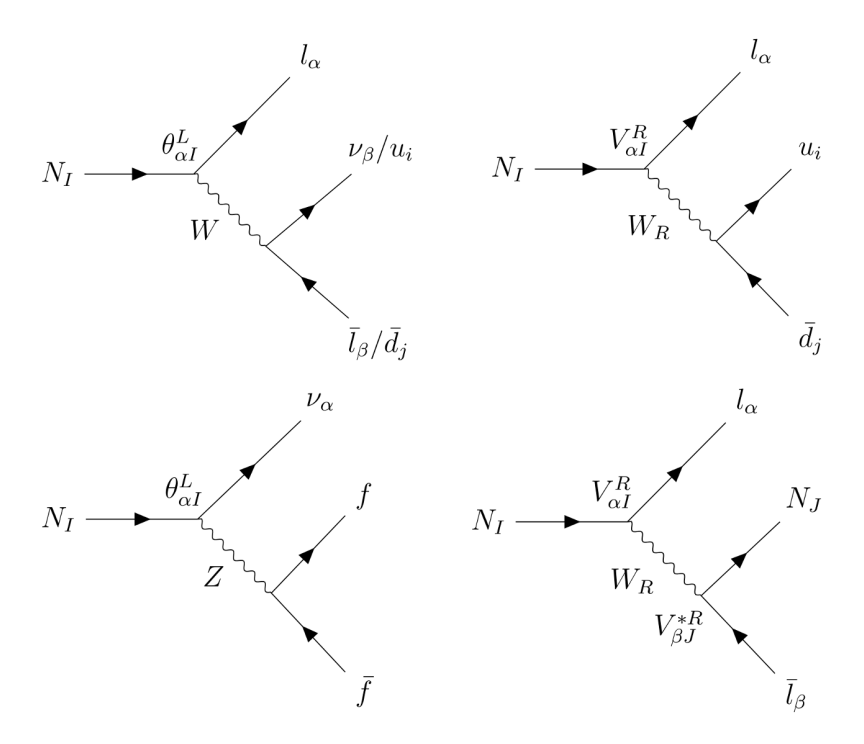


Figure 1. Diagrams of the decay of an HNL. Left: decays through mixing with active neutrinos. The suppression comes from the small mixing angle $\theta_{\alpha I}^L$. Right: decays involving the right-handed interaction. These diagrams are suppressed by $\theta_{\alpha I}^R = V_{\alpha I}^R (m_W/m_{W_R})^2$ at energies below the W_R mass. The bottom-right diagrams have two HNLs while being suppressed by θ^R only once.

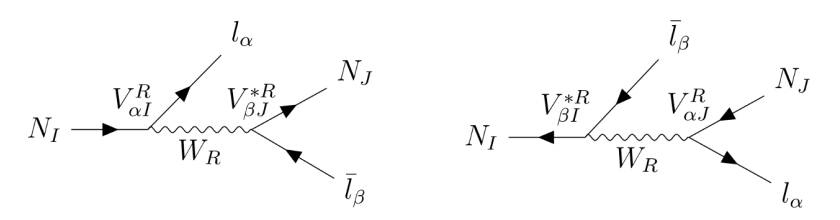


Figure 2. Two interfering diagrams, contributing to the $N_I \to N_J l_\alpha \bar{l}_\beta$ decay. When N_J is produced being ultrarelativistic, the diagrams decouple and correspond to the emission of a specific helicity state.

3 Flavor structure from the seesaw relation

In this section, we derive the numerical values of the V^L , V^R matrices from the seesaw relation, which determines the properties of active neutrinos.

3.1 LRSM Lagrangian

The leptonic Yukawa sector of the LRSM is [98]:

$$\mathcal{L} \supset \bar{L}_{\alpha}([Y_{e}]_{\alpha\beta}\tilde{\Phi} - [Y_{\nu}]_{\alpha\beta}\Phi)R_{\beta} - \frac{1}{2}\bar{L}_{\alpha}^{c}[Y_{1}]_{\alpha\beta}i\sigma_{2}\Delta_{L}L_{\beta} - \frac{1}{2}\bar{R}_{\alpha}^{c}[Y_{2}]_{\alpha\beta}i\sigma_{2}\Delta_{R}R_{\beta} + \text{h.c.}$$
(3.1)

where $L_{\alpha} = (\nu, e_L)_{\alpha}^T$, $R_{\alpha} = (N, e_R)_{\alpha}^T$ are the left and right lepton doublets, $\alpha = e, \mu, \tau$ is the leptonic flavor, $\tilde{\Phi} = \sigma_2 \Phi \sigma_2$ and Φ , Δ_L , Δ_R are scalar fields that acquire the following

vacuum expectation values:

$$\Phi \to v \operatorname{diag}(\cos \beta, -\sin \beta e^{-i\alpha})$$
 $\Delta_{L,R} \to \begin{pmatrix} 0 & 0 \\ v_{L,R} & 0 \end{pmatrix}$

The generalized parity symmetry \mathcal{P} that exchanges the left and right fields $L \leftrightarrow R$, $\Delta_L \leftrightarrow \Delta_R$ implies the following relations:

$$Y_e^{\dagger} = Y_e, \quad Y_{\nu}^{\dagger} = Y_{\nu}, \quad Y_1 = Y_2$$
 (3.2)

After the symmetry breaking, the mass terms in the Lagrangian take the form:

$$\mathcal{L} \supset (m_l)_{\alpha\beta} \bar{e}_{L\alpha} e_{R\beta} - \frac{1}{2} \left(\bar{\nu}^c \ \bar{N} \right) \begin{pmatrix} \frac{v_L}{v_R} M \ M_D^T \\ M_D \ M^* \end{pmatrix} \begin{pmatrix} \nu \\ N^c \end{pmatrix} + \text{h.c.}$$
 (3.3)

with $M = v_R Y_2$ and

$$m_l = vY_e \cos \beta + vY_\nu \sin \beta e^{-i\alpha} \tag{3.4}$$

$$M_D = vY_{\nu}\cos\beta + vY_e\sin\beta e^{-i\alpha} = v\frac{\cos 2\beta}{\cos\beta}Y_{\nu} + m_l^{\dagger}\tan\beta e^{-i\alpha}$$
(3.5)

Diagonalization of the mass terms in the Lagrangian yields the neutrino mass matrix:

$$m_{\nu} = \frac{v_L}{v_R} M - M_D^T (M^*)^{-1} M_D \tag{3.6}$$

To fix the basis, it is most convenient to diagonalize the charged lepton mass matrix m_l . If the scalar sector is CP-conserving, the diagonalization is done via the usual means of a unitary transformation that preserves the form of eqs. (3.4), (3.5). In the general case, however, m_l requires two different unitary matrices for the left and right leptons $L \to E_L L$, $R \to E_R R$, which introduces a unitary matrix $\mathcal{U}_l \equiv E_R^{\dagger} E_L$ to the equations. Without loss of generality, we can fix $E_R = 1$, diagonalize the HNL mass matrix M and define a hermitian matrix Y with the use of a unitary matrix V_R :

$$M \equiv V_R^* m_N^{\mathrm{diag}} V_R^{\dagger}, \qquad Y_{\nu} \frac{\cos 2\beta}{\cos \beta} \equiv V_R Y V_R^{\dagger}$$

The resulting seesaw relation takes the form

$$U_{\text{PMNS}}^* m_{\nu}^{\text{diag}} U_{\text{PMNS}}^{\dagger} = \mathcal{U}_l^T V_R^* \left[\frac{v_L}{v_R} m_N^{\text{diag}} - m_D^T \times (m_N^{\text{diag}})^{-1} \times m_D \right] V_R^{\dagger} \mathcal{U}_l$$
 (3.7)

$$m_D = vY + V_R^{\dagger} m_l^{\text{diag}} \mathcal{U}_l^{\dagger} V_R \cdot \tan \beta \, e^{-i\alpha}$$
(3.8)

where the neutrino mass matrix is written explicitly using the PMNS matrix U_{PMNS} , and the matrix \mathcal{U}_l is defined via the relation

$$\mathcal{U}_l m_l^{\text{diag}} - m_l^{\text{diag}} \mathcal{U}_l^{\dagger} = iv \tan 2\beta \sin \alpha \times V_R Y V_R^{\dagger}$$
(3.9)

To summarize, the set of equations consists of eqs. (3.7)–(3.9) that determine three matrices: the hermitian Y and unitary V_R , \mathcal{U}_l as functions of m_N^{diag} , neutrino masses m_{ν}^{diag} , charge lepton masses m_l^{diag} , the PMNS matrix, and parameters related to the symmetry breaking: the ratio v_L/v_R and angles β , α . Once the equations are solved, the effective couplings that enter eq. (2.1) are given by:

$$\theta_{\alpha I}^{R} = \frac{m_W^2}{m_{W_R}^2} [V^R]_{\alpha I}, \qquad \theta_{\alpha I}^{L} = \frac{(\mathcal{U}_l^T V_R^* m_D^T)_{\alpha I}}{m_{N_I}}$$
 (3.10)

3.2 The approximate symmetry limit

To remind the reader, we are seeking a solution that involves only two degenerate HNLs whose mixing angles significantly exceed the type-I seesaw bound. In the type-I seesaw, one can typically find the closed form for the mixing angles θ^L by employing the Casas-Ibarra parametrization [99]. However, we need to solve the seesaw relation for several variables, i.e., the Dirac mass and V_R , while also ensuring that the Yukawa matrix Y_{ν} is hermitian. An analysis discussing the reconstruction of new physics properties from the seesaw relation can be found in [98, 100–102]. In this work, we employ a different approach, starting by realizing an exact symmetry that makes the mixing angles arbitrarily large without generating neutrino masses. This is achieved by choosing a hermitian Y:

$$m_N^{\text{diag}} = m_N \begin{pmatrix} 0 & 0 & 0 \\ 0 & 1 & 0 \\ 0 & 0 & 1 \end{pmatrix}, \qquad Y = y \begin{pmatrix} 0 & 0 & 0 \\ 0 & 1 & -i \\ 0 & i & 1 \end{pmatrix}, \qquad Y^T (m_N^{\text{diag}})^{-1} Y = 0$$
 (3.11)

Choosing $Y \to Y^T$ simply corresponds to exchanging N_2 and N_3 .

The left-mixing matrix is determined by the right-handed matrix V^R and takes the form

$$\theta_{\alpha I}^{L} = \frac{v}{m_N} (\mathcal{U}_l^T V_R^* Y^T)_{\alpha I} = \frac{\sqrt{2}yv}{m_N} V_L, \qquad U_L \equiv \frac{\sqrt{2}yv}{m_N}$$
$$V_{\alpha 1}^{L} = 0, \qquad V_{\alpha 2} = -iV_{\alpha 3} = \frac{[\mathcal{U}^T V_R^*]_{\alpha 2} + i[\mathcal{U}^T V_R^*]_{\alpha 3}}{\sqrt{2}}$$

We are interested in the case when the mixing angles of N_2 , N_3 exceed the seesaw bound, which implies that $m_N U_L^2 \gg m_{\nu}$. Furthermore, we assume that the type-II contribution to neutrino mass $v_L m_N / v_R$ is much smaller than $m_N U_L^2$ as well. To generate neutrino masses, the exact symmetry should be broken:

$$\kappa \equiv \frac{2v_L}{v_R U_L^2}, \quad m_N^{\text{diag}} = m_N \begin{pmatrix} 0 & 0 & 0 \\ 0 & 1 + \frac{\mu}{2} & 0 \\ 0 & 0 & 1 - \frac{\mu}{2} \end{pmatrix},
m_D = \frac{m_N U_L}{\sqrt{2}} \begin{bmatrix} \begin{pmatrix} 0 & 0 & 0 \\ 0 & 1 & -i \\ 0 & i & 1 \end{pmatrix} + \Delta \end{bmatrix},$$
(3.12)

with small symmetry breaking parameters κ , μ , $|\Delta_{ij}| \ll 1$. The parameter μ controls the relative mass splitting between the two species and can be either positive or negative. The anti-hermitian part of the matrix Δ is subject to the relation with the CP-violating term in eq. (3.8), while the hermitian part is arbitrary at this point.

In the linear order in terms of the introduced small parameters, eq. (3.7) becomes:

$$U_{\text{PMNS}}^* m_{\nu}^{\text{diag}} U_{\text{PMNS}}^{\dagger} = -\mathcal{U}_l^T V_R^* X V_R^{\dagger} \mathcal{U}_l$$
 (3.13)

where X has the following form:

$$X = \frac{m_N U_L^2}{2} \begin{pmatrix} 0 & \epsilon_1 & -i\epsilon_1 \\ \epsilon_1 & \epsilon_2 + \epsilon_3 & -i\epsilon_3 \\ -i\epsilon_1 & -i\epsilon_3 & \epsilon_2 - \epsilon_3 \end{pmatrix}$$
(3.14)

with complex parameters ϵ_i , i=1,2,3, whose definitions are given in appendix B. The form of the perturbation matrix X automatically ensures that the lightest eigenvalue of the neutrino mass matrix is zero. The other two eigenvalues must be equal to the neutrino masses, which are fixed by the measured neutrino mass splittings. We adopt the definition in which $m_{\nu}^{\text{diag}} = \text{diag}(0, m_2, m_3)$ is the mass-ordered diagonal matrix of active neutrinos with masses:

$$m_2 = \sqrt{\Delta m_{21}^2} \approx 9 \text{ meV}$$
 $m_3 = \sqrt{\Delta m_{31}^2} \approx 50 \text{ meV},$ (NH)
 $m_2 = \sqrt{|\Delta m_{31}^2|} \approx 50 \text{ meV}$ $m_3 = \sqrt{|\Delta m_{31}^2| + \Delta m_{21}^2} \approx 51 \text{ meV},$ (IH) (3.15)

and, for convenience, we define the PMNS matrix in the mass-ordered basis:

$$U_{\text{PMNS}} = \tilde{U}_{\text{PMNS}} P \begin{pmatrix} 1 & 0 & 0 \\ 0 & e^{i\eta} & 0 \\ 0 & 0 & 1 \end{pmatrix}, \quad P = \begin{pmatrix} 0 & 1 & 0 \\ 0 & 0 & 1 \\ 1 & 0 & 0 \end{pmatrix} \text{ for IH; } P = 1_{3\times3} \text{ for NH}$$
 (3.16)

where \tilde{U}_{PMNS} is the experimentally measured matrix as given explicitly in [103]. In this parameterization, η is the single Majorana phase associated with m_2 , and the matrix P reorders neutrino states to the conventional ordering.

If the complex ϵ_i parameters can vary independently, the full explicit 4-parameteric solution for the matrix $X = e^{i\phi_0}W^T \operatorname{diag}(0, m_2, m_3)W$ that yields the correct eigenvalues is:

$$X = e^{i\phi_0} \frac{m_2 + m_3}{2} \begin{pmatrix} 0 & \frac{e^{i\phi_2}}{\sqrt{2}} s_{2\gamma} s_{\psi} & -\frac{e^{i\phi_2}}{\sqrt{2}} s_{2\gamma} s_{\psi} \\ \frac{e^{i\phi_2}}{\sqrt{2}} s_{2\gamma} s_{\psi} & s_{2\gamma} c_{\psi} + e^{i\phi_1} c_{2\gamma} & -ie^{i\phi_1} c_{2\gamma} \\ -\frac{e^{i\phi_2}}{\sqrt{2}} s_{2\gamma} s_{\psi} & -ie^{i\phi_1} c_{2\gamma} & s_{2\gamma} c_{\psi} - e^{i\beta} c_{2\gamma} \end{pmatrix},$$
(3.17)

where ψ , ϕ_i are free parameters, the angle γ is defined via $\tan \gamma = \sqrt{m_2/m_3}$, and the unitary matrix W is:

$$W(\psi, \phi_1, \phi_2) = \frac{e^{-\frac{i\phi_1}{2}}}{\sqrt{2}} \begin{pmatrix} \sqrt{2}e^{i\phi_2}c_{\psi} & -s_{\psi} & -is_{\psi} \\ -i\sqrt{2}e^{i\phi_2}c_{\gamma}s_{\psi} & -ic_{\gamma}c_{\psi} + ie^{i\phi_1}s_{\gamma} & c_{\gamma}c_{\psi} + e^{i\phi_1}s_{\gamma} \\ -\sqrt{2}e^{i\phi_2}s_{\gamma}s_{\psi} & -s_{\gamma}c_{\psi} - e^{i\phi_1}c_{\gamma} & -is_{\gamma}c_{\psi} + ie^{i\phi_1}s_{\gamma} \end{pmatrix} (3.18)$$

using the notation $s_x \equiv \sin x$, $c_x \equiv \cos x$.

The matrix of right-handed couplings V^R becomes:

$$V^{R} = ie^{\frac{i\phi_0}{2}} \mathcal{U}_l U_{\text{PMNS}} W(\psi, \phi_1, \phi_2)$$
(3.19)

where the matrix \mathcal{U}_l turns out to be, in the linear approximation, independent of any of the parameters ψ , ϕ_i , and is given, according to eq. (3.9), as the solution to the equation:

$$m_l^{\text{diag}} \mathcal{U}_l - \mathcal{U}_l^{\dagger} m_l^{\text{diag}} = i \frac{m_N U_L}{\sqrt{2}} t_{2\beta} s_{\alpha} \times U_{\text{PMNS}} \begin{pmatrix} 0 & 0 & 0\\ 0 & 2s_{\gamma}^2 & -is_{2\gamma}\\ 0 & is_{2\gamma} & 2c_{\gamma}^2 \end{pmatrix} U_{\text{PMNS}}^{\dagger}$$
(3.20)

The anti-hermitian correction to the Dirac mass $\Delta^A \equiv (\Delta - \Delta^{\dagger})/2$ must satisfy, according to eq. (3.8):

$$\Delta^{A}(\psi, \phi_{1}, \phi_{2}) = \frac{t_{\beta}}{\sqrt{2}m_{N}U_{L}} \times W^{\dagger}U_{\text{PMNS}}^{\dagger} \cdot [\mathcal{U}_{l}^{\dagger}m_{l}^{\text{diag}}e^{-i\alpha} - m_{l}^{\text{diag}}\mathcal{U}_{l}e^{i\alpha}] \cdot U_{\text{PMNS}}W$$
 (3.21)

independent of the angle ϕ_0 . Because of this additional constraint, the assumption that the parameters ϵ_i in eq. (3.14) are independent is, in fact, incorrect. As shown in appendix B, this constraint can be incorporated in the parametrization by fixing the angle ϕ_0 according to:

$$\sin \phi_0(\psi, \phi_1, \phi_2) = \frac{m_N U_L^2}{m_2 + m_3} \times \frac{\operatorname{Im}(\Delta_{22}^A + \Delta_{33}^A) - \operatorname{Re}(\Delta_{23}^A - \Delta_{32}^A)}{s_{2\gamma} c_{\psi}}$$
(3.22)

This angle only enters the couplings V^R , V^L in the form of an overall phase and, therefore, its exact numerical value is irrelevant. However, since the sine function is bounded, this expression turns into a constraint on the anti-hermitian component Δ^A , which must not generate too large neutrino masses. This limits the amount of CP-violation that can be produced by either small β or α . To study the bound on this quantity, we need to carefully expand Δ^A , employing the definition of \mathcal{U}_L (3.20):

$$\begin{split} \Delta^A(\psi,\phi_1,\phi_2) &\approx t_\beta s_\alpha \Bigg[-i \cdot \frac{\sqrt{2}}{m_N U_L} W^\dagger U_{\text{PMNS}}^\dagger m_l^{\text{diag}} U_{\text{PMNS}} W - \frac{t_{2\beta}}{2} \begin{pmatrix} 0 & 0 & 0 \\ 0 & 1 & -i \\ 0 & i & 1 \end{pmatrix} \\ &+ O\left(\frac{m_N U_L}{m_e} \beta s_\alpha\right) \Bigg] \end{split}$$

The second term, scaling as $O(\beta^2 \alpha)$, vanishes identically in the numerator of eq. (3.22) and can be ignored. The first term generally does not exhibit such cancellation, resulting in the following bound:

$$\beta s_{\alpha} \lesssim \frac{m_2 + m_3}{m_{\tau} U_L} < 10^{-5} \sqrt{\frac{10^{-10}}{U_L^2}}$$
 (3.23)

For consistency, the expansion parameter of the further series must be small, implying:

$$\frac{m_N U_L}{m_e} \beta s_\alpha \ll 1 \quad \Longrightarrow \quad m_N \ll 10^7 \,\text{GeV} \tag{3.24}$$

which is satisfied in the mass range we are interested in. This inequality also implies that the matrix \mathcal{U}_l deviates from unity at a level much smaller than $m_N/10^7$ GeV.

The obtained bound on the amount of CP-violation is much stricter than constraints from experiments that search for mixing between the charged W and W_R bosons, expected with the angle $2\beta (m_W/m_{W_R})^2$ [104] and excluded down to 0.01 - 0.1 [105, 106], as well as the limits on the amount of CP-violation in the quark sector $\beta \sin \alpha \lesssim m_b/m_t$ [95, 107, 108].

There are further constraints, relying on the assumptions regarding the properties of the DM candidate N_1 . Small perturbations in the Dirac mass are responsible for the generation of the mixing angle U_1^L :

$$(U_1^L)^2 \equiv \sum_{\alpha=1,2,3} |\theta_{\alpha 1}^L|^2 = \frac{m_N^2 U_L^2}{2m_{N_1}^2} \sum_{\alpha=1,2,3} |\Delta_{1\alpha}|^2$$
(3.25)

which is subject to astrophysical constraints [54]. This formula implies the following inequality, proven in appendix B:

$$\left[\frac{m_{N_1}U_1^L}{m_N U_L}\right]^2 \ge \frac{|\Delta_{11}^A|^2}{2} + \left|\frac{m_2 + m_3}{2\sqrt{2}m_N U_L^2} s_{2\gamma} s_{\psi} e^{-i(\phi_2 + \phi_0)} - 2(\Delta_{12}^A + i\Delta_{13}^A)\right|^2.$$
(3.26)

Dismissing possible cancellations, we can set rough limits on the parameters:

$$|\sin \psi| \lesssim \frac{m_{N_1} U_L U_L^1}{m_2 + m_3} \qquad \lesssim \sqrt{\frac{U_L^2}{10^{-3}}} \times \left(\frac{m_{N_1}}{1 \text{ keV}}\right)^{-\frac{3}{2}}$$

$$t_\beta s_\alpha \lesssim \frac{m_{N_1} U_L^1}{m_\tau} \qquad \lesssim 10^{-9} \times \left(\frac{m_{N_1}}{1 \text{ keV}}\right)^{-\frac{3}{2}}$$
(3.27)

$$t_{\beta} s_{\alpha} \lesssim \frac{m_{N_1} U_L^1}{m_{\tau}} \qquad \lesssim 10^{-9} \times \left(\frac{m_{N_1}}{1 \text{ keV}}\right)^{-\frac{3}{2}}$$
 (3.28)

assuming a conservative bound $(U_1^L)^2 < 10^{-5} (m_{N_1}/1 \,\text{keV})^{-5}$ consistent with X-ray observations [54] in the keV mass range for m_{N_1} . The ψ constraint implies that this angle is negligibly small for virtually all HNL masses below the electroweak scale, given the current experimental limits on U_L^2 [6]. The bound (3.28) on the CP-violating angles is somewhat stricter than that of eq. (3.23). However, it relies on the assumptions about the DM.

To recapitulate, the matrices V_L , V_R are:

$$V^{R} = ie^{i\frac{\phi_0}{2}} \mathcal{U}_l U_{\text{PMNS}} W(\psi, \phi_1, \phi_2), \tag{3.29}$$

$$V_{\alpha 2}^{L} = -iV_{\alpha 3}^{L} = i e^{-i\frac{\phi_0 + \phi_1}{2}} \begin{bmatrix} \tilde{U}_{\text{PMNS}}^* P \times \begin{pmatrix} 0 \\ ie^{-i\eta} s_{\gamma} \end{pmatrix} \end{bmatrix}_{\alpha}, \tag{3.30}$$

with W defined in eq. (3.18), the PMNS matrix in eq. (3.16). The flavor coupling matrices V_R , V_L depend on five unknown parameters: the Majorana phase η of the PMNS matrix, the amount of CP-violation $\beta \sin \alpha$ that controls \mathcal{U}_L via eq. (3.20), and the three angles ψ, ϕ_1, ϕ_2 . The requirement of self-consistency of the seesaw relation limits the amount of CP-violation and, for HNL mass in the GeV-TeV scale, renders the matrix \mathcal{U}_l equal to unity. Somewhat more tentative assumptions regarding the DM candidate N_1 also limit the parameter ψ , further compressing the parameter space of possible couplings. The coupling matrices have the following properties:

- The magnitudes of the LH couplings $|V_L|$ depend only on η and coincide with those of the Casas-Ibarra parameterization in the pure type-I seesaw with the approximate symmetry limit.
- The magnitudes of RH couplings $|V_{\alpha 1}^R|$ of the DM candidate depend only on ψ and are reduced to fixed values at vanishing ψ .
- The RH couplings $|V_{\alpha I}^R|$ for the heavy N_2 , N_3 species depend on η , ϕ_1 , and ψ .

In the limit $\psi \to 0$, the RH couplings of the DM candidate become fixed at

$$|V_{\alpha 1}^{R}|^{2} = |\tilde{U}_{\alpha 1}^{\text{PMNS}}|^{2} = \begin{cases} \left(0.68_{-0.04}^{+0.03}, \ 0.07_{-0.02}^{+0.18}, \ 0.24_{-0.18}^{+0.03}\right), & \text{NH} \\ \left(0.022_{-0.002}^{+0.002}, \ 0.57_{-0.17}^{+0.04}, \ 0.41_{-0.04}^{+0.17}\right), & \text{IH} \end{cases}$$
(3.31)

where the errors correspond to the 3σ confidence intervals of the neutrino oscillation parameters [109] (excluding the Super-Kamiokande data).

Thanks to the unitarity of the matrix V^R , the following combination of the degenerate pair's couplings is fixed:

$$\frac{|V_{\alpha 2}^R|^2 + |V_{\alpha 3}^R|^2}{2} = \frac{1 - |V_{\alpha 1}^R|^2}{2} \equiv \langle V_{\alpha}^R \rangle^2 = \begin{cases} \left(0.16_{-0.02}^{+0.02}, \ 0.47_{-0.09}^{+0.01}, \ 0.38_{-0.02}^{+0.09}\right), & \text{NH} \\ \left(0.489_{-0.001}^{+0.001}, \ 0.22_{-0.02}^{+0.09}, \ 0.30_{-0.09}^{+0.02}\right), & \text{IH} \end{cases}$$
(3.32)

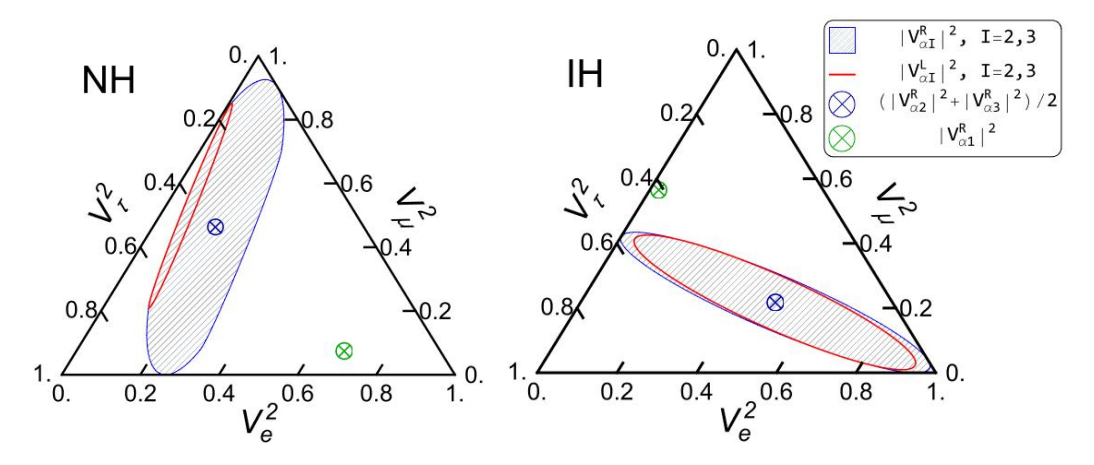


Figure 3. Ternary plots for the couplings $|V^L|^2$, $|V^R|^2$ with approximate symmetry in the limit $\mathcal{U}_l \to 1$, $\psi \to 0$, for the normal (left) and inverse (right) neutrino hierarchies. The red lines show the range of possible values of the LH couplings $|V_{\alpha 2}^L|^2 = |V_{\alpha 3}^L|^2$. The green cross shows a fixed value of the RH couplings $|V_{\alpha 1}^R|$ of the DM candidate, given by eq. (3.31). The dashed blue region represents the range of the values for $|V_{\alpha 2}^R|^2$, $|V_{\alpha 3}^R|^2$. The corresponding pairs of points are located symmetrically around the blue cross, which depicts the fixed value of $\langle V_{\alpha}^R \rangle^2 \equiv (|V_{\alpha 2}^R|^2 + |V_{\alpha 3}^R|^2)/2$, see eq. (3.32). The plot uses the best-fit neutrino oscillation parameters [109] (without the SK data) and does not include the corresponding experimental uncertainties.

The summarizing ternary plots of the values of V_L , V_R for $\psi = 0$ are shown in figure 3, while the effect of nonzero ψ is shown in figure 4.

4 Experimental probes

In this section, we analyze various experimental probes that may be used to gain insights into the internal structure of the model. We assume that the coupling matrices V^R , V^L are given by eqs. (3.29), (3.30), with $\psi = 0$, $\mathcal{U}_l = 1$. The left couplings V^L depend only on the Majorana phase η , while V^R depends on two parameters: η and ϕ_1 .

4.1 Sensitivity of FCC-ee in the Z-pole mode

The best sensitivity to heavy neutral leptons in the ν MSM in the $\sim 10-100\,\mathrm{GeV}$ mass range is offered by the FCC-ee, operating at the Z-pole mass [21, 110], thanks to the abundant sample of more than 10^{12} Z-bosons. The production of N in the decay of Z-boson occurs through either the $Z \to N\nu$ process, mediated by the left-handed interaction, or by mixing between Z and a possible heavy state Z_R , which would enable the $Z \to NN$ decay. Our analysis focuses on the properties of fermions and has been largely independent of the details of the bosonic sector of the model, only relying on the existence of W_R . The process $Z \to NN$, however, does require model-dependent details. Even without this production channel, nonminimal interactions may be probed by their effect on the HNL decays. Additional interactions may enhance the signal rate to the observable level in parts of the parameter space otherwise unreachable. This refers specifically to the light HNLs with small coupling constant U_L^2 , for which the decay length reaches macroscopic values in the LH-only case and suppresses the

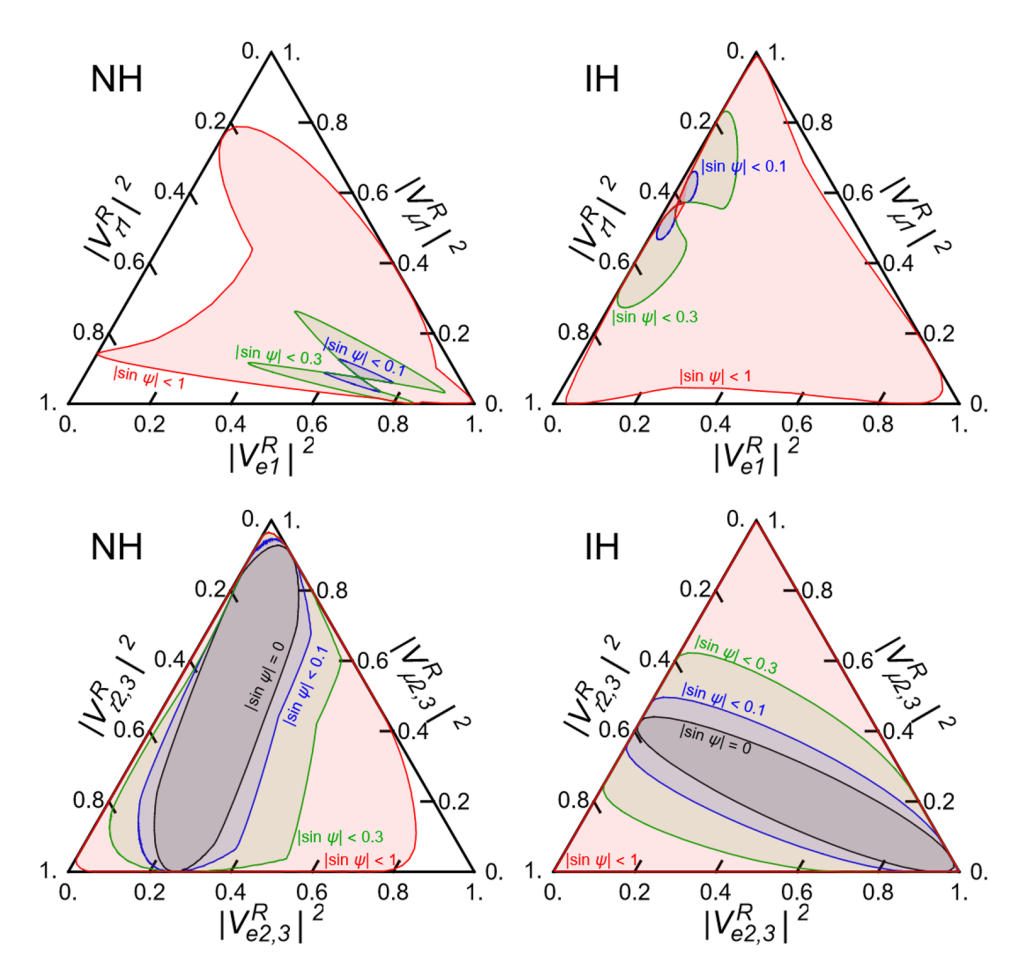


Figure 4. The effect of the ψ parameter on the $V_{\alpha 1}^R$ (top) and $V_{\alpha 2,3}^R$ (bottom) couplings for the normal (left) and inverted (right) neutrino hierarchy. The left couplings V_L remain unchanged. The constraints on ψ rely on the assumptions on the DM candidate; for a keV-scale N_1 , ψ is negligibly small for HNL masses in the GeV-TeV range, except for a narrow strip above the electroweak scale where $N_{2,3}$ with large mixing angles $U_L^2 \gtrsim 10^{-3}$ are not excluded.

probability of the decay within the detector system. With the new interaction, the decay width is increased, forcing HNLs to decay faster.

To estimate the sensitivity of an experiment, hosted by FCC-ee, let us provide simple scaling arguments. At the lower bound of sensitivity [111], the number of events is proportional to:

$$N_{\rm ev} \propto \underbrace{\left[U_L^2 {\rm Br}_{Z \to \nu N} + c_Z U_R^2 {\rm Br}_{Z \to N N}\right]}_{\rm production} \times \underbrace{\left[U_L^2 \cdot {\rm Br}_{{\rm vis.},L} + U_R^2 \cdot {\rm Br}_{{\rm vis.},R}\right]}_{\rm decay\ width}$$
 (4.1)

where the production branchings

$$Br_{Z \to \nu N} = \left(1 - \frac{m_N^2}{m_Z^2}\right)^2 \left(1 + \frac{m_N^2}{2m_Z^2}\right)$$
$$Br_{Z \to NN} = \left(1 - \frac{m_N^2}{m_Z^2}\right) \sqrt{1 - \frac{4m_N^2}{m_Z^2}}$$

carry the kinematic dependence on the HNL mass, while $\operatorname{Br}_{\operatorname{vis},L(R)}$ stands for the visible branching ratio for the pure left(right)-handed interactions. The parameter c_Z contains the ZNN couplings and in the minimal LRSM is given by [112]:

$$c_Z = \frac{1}{4} \frac{\cos^4 2\theta_W}{\cos^4 \theta_W} \approx 0.04$$

This parameter is quite small. If the production is dominated by the $Z \to NN$ decay, the decay width is also dominated by U_R^2 and the LH interaction can be neglected. If $U_R \lesssim U_L$, both production and decay are dominated by LH interactions. Nevertheless, there exists a region in the parameter space between:

$$\frac{U_L^2}{c_Z} \frac{\operatorname{Br}_{Z \to \nu N}}{\operatorname{Br}_{Z \to NN}} \gtrsim U_R^2 \gtrsim U_L^2$$

where production and decay become parametrically independent.

For a more rigorous analysis of the FCC-ee sensitivity to heavy neutral leptons, we use the setup described in [21], with the expected $5 \cdot 10^{12}~Z$ -bosons. Specifically, we assume the CLD design, with the geometry of a cylinder with length 8.6 m and radius 5 m. Four decay events with the displacement from the HNL production point exceeding $400~\mu m$ are required.

For the sake of generality, we neglect the masses of the charged leptons and u,d,s,c quarks, and also neglect the decay of HNLs into a b-quark. The last assumptions can safely be done for $N \to lq_ub$ decays thanks to the smallness of ub and sb entries of the CKM matrix. For the neutral current decays $N \to \nu bb$, however, this can lead to an error of the order at most 5% level in the decay width. Finally, we assume that cross-HNL decays $N_I \to N_J l_\alpha l_\beta$ are absent and only one HNL species is produced. These assumptions, having a minor effect on the results, allow us to eliminate the flavor-specific details and build general bounds which are valid for any combinations of $V_{\alpha I}^{L/R}$.

Under these assumptions, the full decay width can be approximated as

$$\Gamma_{L/R} = 2U_{L,R}^2 \times C_{L/R} \times \frac{G_F^2 m_N^5}{192\pi^3},$$

where the prefactor 2 counts the charge-conjugated decay modes for a Majorana fermion. The coefficients are

$$C_R = 6,$$
 $C_L = \frac{1}{12}(153 - 84\sin^2\theta_W + 152\sin^4\theta_W) = 11.8$

The decay width of the only invisible mode is $\Gamma(N \to 3\nu) = 2U_L^2 \times G_F^2 m_N^5 / (192\pi^3)$. The final needed piece of information is HNL momentum, which determines the decay length:

$$p_{N} = \frac{m_{Z}}{2} \begin{cases} 1 - m_{N}^{2} / m_{Z}^{2}, & Z \to \nu N \\ \sqrt{1 - 4m_{N}^{2} / m_{Z}^{2}}, & Z \to N N \end{cases}$$

The sensitivity of FCC-ee to HNLs is shown in figure 5. For smaller mixing angles and masses below 30 GeV, the LH sensitivity drops due to the large lifetime of HNLs. The RH interactions mediated by W_R with mass $20-40\,\text{GeV}$ improve the sensitivity to U_L in this region by forcing the particles to decay promptly. For small U_L^2 and masses above 30 GeV, the particle lifetime is sufficiently small, and the sensitivity is saturated by the production limit.

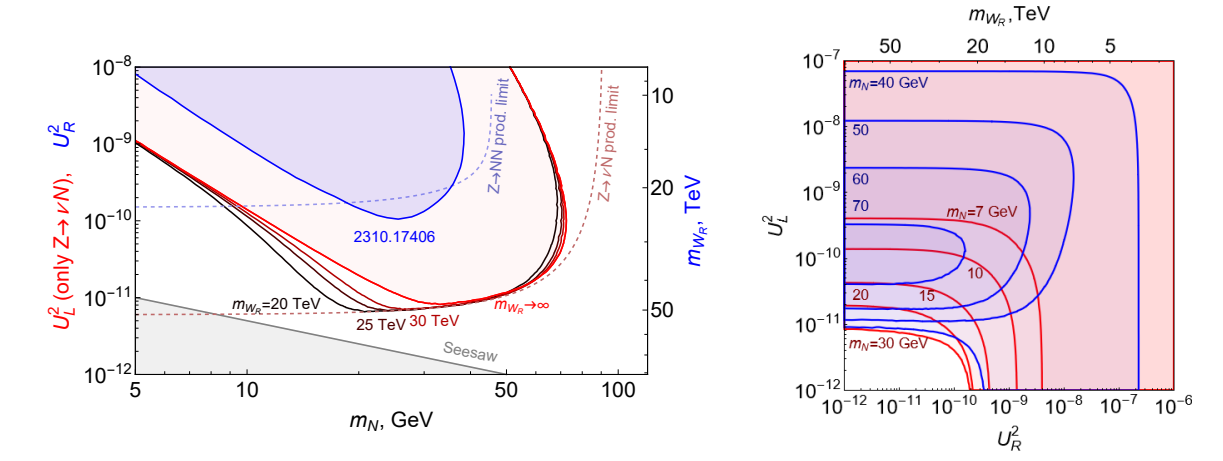


Figure 5. Left: sensitivity contours for U_L^2 (red-shaded lines), assuming HNL production only in $Z \to \nu N$ decays. The filled red $m_{W_R} \to \infty$ region is the sensitivity in the model with only left-handed interactions. Below the dashed light-red line denoted as Z prod limit in the U_L^2 parameter space, the number of produced HNLs is less than four. With W_R masses around $20-40\,\mathrm{TeV}$, the sensitivity to small U_L^2 in the HNL mass range $20-30\,\mathrm{GeV}$ improves at the lower bound. For smaller W_R mass, RH starts to dominate, as demonstrated by the proper sensitivity reach to U_R^2 (blue line) from [113] (one displaced vertex, PMNS mixing), which includes all production channels. The light-blue line corresponds to the production limit from $Z \to NN$ in the U_R^2 space. Right: estimated sensitivity contours in the (U_L^2, U_R^2) space for various choices of the HNL mass, from 7 GeV to 70 GeV, including both $Z \to \nu N$ and $Z \to NN$ decay channels with $c_Z = 0.04$.

4.2 (De)coherence of the quasi-degenerate pair

Observation of lepton number violating (LNV) processes in collider experiments would be a smoking gun for new physics, as illustrated by the famous Keung-Senjanovic process [97] in searches for the LRSM right-handed neutrinos. Lepton number violation is closely linked to leptogenesis and the nature of active neutrino masses, which, if Majorana, should manifest themselves in $0\nu\beta\beta$ decays [114]. In the scenario of quasi-degenerate HNLs, LNV happens due to oscillations between the lepton and antilepton-like parts of the pair. The analysis of the properties of these oscillations and various collider probes can be found in [115–119]. If one of the two SM leptons, required to establish LNV directly, escapes detection in the form of a neutrino at lepton colliders [120, 121] or by being absorbed in the target in case of beam dump experiments [122], kinematic information about the HNL decay products may still be used to probe the nature of HNLs. Although oscillations are believed to be directly defined by the innate properties of the new particles (namely, mass splitting), ref. [123] points out that dynamical effects, arising from the uncertainty of particle energy, may also contribute to decoherence between the two species and spoil the connection between the observed LNV and particle parameters. In what follows, we study the properties of HNL interactions in two limits, assuming that the oscillations are either very slow or very fast and treating this choice as an independent model parameter.

At the moment of creation of an HNL, the two species are produced in a superposition. If the oscillations between them are too rapid compared to the lifetime, the superposition becomes decoherent: an observable signal may be computed simply as a sum of two independent contributions. If the oscillations are sufficiently slow, the two species remain coherent and interfere with each other, altering the decay pattern of the resulting state due to interference. In the pure left-handed case, the probability of observing final states that violate lepton number conservation vanishes as a manifestation of the approximate symmetry of the HNL pair. The situation becomes more complicated for the right-handed interactions, as they do not respect the imposed approximate lepton symmetry, which is attributed only to the specific choice of the Dirac mass matrix without any particular symmetry-driven restrictions on V^R .

Below, we analyze the coherent and decoherent cases. For simplicity, we assume a hierarchical relation between the small couplings U_L^2 , U_R^2 , such that the two interactions do not mix in production/decay. We assume that an HNL is produced together with a lepton of flavor α , and interacts with a β -flavored (anti)lepton.

(a) Rapid decoherence.

If the two HNLs are treated as independent particles, the total number n_I of HNLs created with the α lepton flavor is simply proportional to $|V_{\alpha I}|^2$ with V standing for either V^R or V^L , depending on the type of interactions. Each of the HNLs then decays into β -flavored leptons and antileptons independently with equal probabilities.

The number of events $n_{\alpha\beta}$ $(n_{\alpha\bar{\beta}})$ with l_{α} accompanying the HNL production and l_{β} (\bar{l}_{β}) in the final state is given, up to the overall normalization, by the matrix:

$$n_{\alpha\beta} = n_{\alpha\bar{\beta}} \propto P_{\alpha} D_{\beta} (|V_{\alpha 2}|^2 |V_{\beta 2}|^2 + |V_{\alpha 3}|^2 |V_{\beta 3}|^2) \tag{4.2}$$

where P_{α} and D_{β} are kinematic factors that carry the dependence on the mass of the charged lepton. The kinematic matrix $P_{\alpha}D_{\beta}$ is therefore determined by the particle mass (measured by some other means) and the experimental setup, which may have different acceptance and detection efficiencies for different leptons. In the case of LH interactions, there is no difference between I=2,3, resulting in the standard product $|V_{\alpha 2}^L|^2 \cdot |V_{\beta 2}^L|^2$, which depends only on the Majorana phase η and the neutrino mass hierarchy. In the RH case, the expression in the brackets depends explicitly on the internal model parameters: phases η and ϕ_1 .

(b) Coherent pair.

In the opposite scenario, the pair remains coherent. In the sequential process of HNL production and decay, the intermediate wave function is a mixture of N_2 and N_3 . The combined wave function created after the interaction is determined by the corresponding currents:

$$\begin{split} J_{L,\alpha} &\propto V_{\alpha 2}^L \bar{l}_{\alpha} (N_2^c - i N_3^c) + \text{h.c.} \\ J_{R,\alpha} &\propto V_{\alpha 2}^R \bar{l}_{\alpha} N_2 + V_{\alpha 3}^R \bar{l}_{\alpha} N_3 + \text{h.c.} \end{split}$$

and the matrix of the number of events with different lepton flavors gets the following form:

$$n_{\alpha\bar{\beta}} \propto P_{\alpha} D_{\beta} |V_{\alpha 2} V_{\beta 2}^* + V_{\alpha 3} V_{\beta 3}^*|^2$$
 (LNC)

$$n_{\alpha\beta} \propto P_{\alpha}D_{\beta}|V_{\alpha2}V_{\beta2} + V_{\alpha3}V_{\beta3}|^2$$
 (LNV)

	Decoherent case	Coherent case
R prod., R decay	LNC, LNV	LNC, LNV
L prod., R decay	LNC, LNV	LNV + LNC

Table 1. Event matrices that reduce to the same parametric form of eq. (4.5) after summation over the initial lepton flavor α . For LH production and RH decay, the relation only holds for the sum of the lepton number violating and conserving decays; in all other cases, the relation holds for both types separately.

For LH interactions $V_{\alpha 2}^L = -iV_{\alpha 3}^L$, the standard result is the absence of a lepton number violation in the final state. For RH interactions, both matrices are always nonzero.

In the case of right-handed production and decay, the matrices may be simplified to:

$$n_{\alpha\bar{\beta}} \propto P_{\alpha} D_{\beta} |\delta_{\alpha\beta} - [U_{\text{PMNS}}]_{\alpha 1} [U_{\text{PMNS}}]_{\beta 1}^{*}|^{2}$$
(4.3)

$$n_{\alpha\beta} \propto \frac{P_{\alpha}D_{\beta}}{(m_2 + m_3)^2} \left| \left(U_{\text{PMNS}}^* \begin{pmatrix} 0 & 0 & 0 \\ 0 & -i\sqrt{m_2 m_3} & m_3 - m_2 \\ 0 & m_3 - m_2 & -i\sqrt{m_2 m_3} \end{pmatrix} U_{\text{PMNS}}^{\dagger} \right)_{\alpha\beta} \right|^2$$
 (4.4)

with the PMNS matrix given by eq. (3.16).

If the pair remains coherent, the dependence of the event matrices on the parameter ϕ_1 vanishes as a result of the underlying symmetry between the two HNLs. The Majorana phase η only affects the matrix of LNV events, while the LNC event matrix is fixed.

In some experimental setups, the initial lepton l_{α} may escape detection. This applies to FCC-ee in the Z-pole mode, where the HNL can be produced in $Z \to \nu N$ decays with an unobservable neutrino, and for beam-dump experiments, in which all production-related information gets lost in the target. In this case, the event matrices must be summed up over $\alpha + \bar{\alpha}$. If the kinematics factors P_{α} are equal for all lepton flavors, most of the event matrices are reduced to the same parametric dependence thanks to the unitarity of V^R :

$$\sum_{\alpha} n_{\alpha\beta} \propto D_{\beta}(|V_{\alpha 2}^{R}|^{2} + |V_{\alpha 3}^{R}|^{2}), \quad \text{if } P_{\alpha} = \text{const}$$
(4.5)

proportional to the averaged couplings $\langle V_{\alpha}^R \rangle^2$ of eq. (3.32), which are fixed for a given neutrino hierarchy. The list of matrices that reduce to this relation is given in table 1. In other words, all the internal information of the models vanishes, and the apparent experimental signal is equivalent to the one from a single HNL with a very specific set of couplings, determined only by the neutrino mass hierarchy. This can be used as a perfect benchmark model of quasi-degenerate HNLs within the minimal seesaw scenario of section 3.2. For the nonminimal seesaw scenarios, the same result (4.5) holds with the appropriate values of $(V_{\alpha}^R)^2$, which are no longer fixed.

Let us now discuss the implications of the results for the event matrices for differentiating between the coherent and decoherent cases. First, let us start with the mentioned FCC-ee in the Z-pole regime, specifically the $Z \to \nu N$ channel. The neutrino in the $Z \to \nu N$ decay cannot be detected. Therefore, neither the associated lepton flavor nor charge can be identified. If the decay of an HNL happens through the RH interaction, one can compare the probabilities

to have different lepton flavors with the concrete prediction of eq. (4.5). If the experimental results do agree with the model, it becomes significantly more challenging to establish the nature of the new fermions. A possible solution is to employ the nonzero polarization of the Z-bosons and the resulting features in the kinematic distribution of the final lepton [124] Another possibility consists of observing oscillations directly as time-dependent variance in the properties of the HNLs [120]. For decays $Z \to NN$, both charged leptons in the final state can be observed, providing a direct test of lepton number violation.

At SHiP, oscillations lead to position-dependent features in the kinematic distributions of decay products [122]. These features can be observed if the oscillation length is of the 1 m scale, comparable to the size of the experiment. Otherwise, one has to rely directly on the event matrices in order to probe the nature of HNLs. New physics particles are produced inside the target, propagate to the decay vessel, and decay into a charged lepton and hadrons. The measurement of particle mass is possible by studying the kinematics of the decay products. Absence of purely leptonic decays would indicate that the right-handed interactions are dominant. The summation of the event matrix over the unobserved initial lepton flavor α loses some information, but not as drastically as eq. (4.5) suggests, if the HNL mass is around a few GeV, which is the mass range relevant for beam-dump experiments. For a concrete example, we consider HNLs with a mass of 1 GeV: the main production channel is decays $D_{(s)}^{\pm} \to X l^{\pm} N$ of D-mesons, produced in the proton scatterings. For this mass, tau-leptons cannot be produced kinematically, $P_{\tau} = D_{\tau} = 0$, while electrons and muons are approximately equivalent: $P_e \approx P_\mu$, $D_e \approx D_\mu$ up to small corrections due to the muon mass. Assuming that these leptons are detected with a unit efficiency, the theoretical prediction of the fraction $N_e/(N_e + N_\mu)$ of events with an electron in the final state to events with either electron or muon can be computed directly. For the decoherent case, the range of values that the ratio can take is somewhat larger than that of the coherent case. Figure 6 shows the results for $N_e/(N_e+N_\mu)$; if the experimental measurement lies outside of the range defined by the blue bands (outside the dashed region), the coherent case in the minimal scenario is excluded.

At hadron colliders, the Keung-Senjanović process $pp \to Xl_{\alpha}N \to Xl_{\alpha}(Yl_{\beta})$ is a powerful probe since both leptons can be traced, and the event matrix can be fully reconstructed. Misidentification of which lepton is initial and which one is final, a possible issue for short-lived HNLs, does not lose any information, since the event matrices are symmetric. With the twelve independent entries of $n_{\alpha\beta}$ and $n_{\alpha\bar{\beta}}$, a full fit of the model can be performed in the standard way. For the sake of simplicity, we focus on the relation between the lepton number violating same-sign (SS) versus conserving opposite-sign (OS) events. We assume that lepton masses can be neglected and consider only the coherent case, since the lepton number conserving/violating events for the decoherent case are trivially expected to occur with equal probability. The relative fractions of SS and OS to the total number of events as functions of the Majorana phase η for different combinations of lepton flavors are shown in figure 7. The fractions of OS events are fixed and can be used to check the consistency of the model. The SS events provide information on η .

At *lepton colliders*, the unified low-energy phenomenology described in section 2 is not valid. The analysis of LRSM at lepton colliders can be found in ref. [113]. Two main differences that have to be taken into account are: HNL production through the neutral

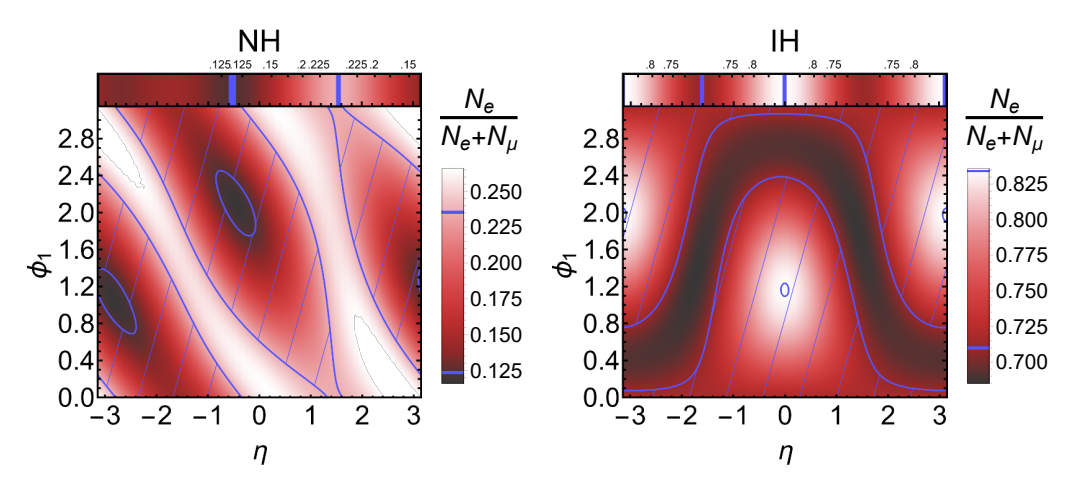


Figure 6. The fraction $N_e/(N_e+N_\mu)$ of observed decays into e versus decays in either e or μ as a function of η , ϕ_1 for the normal (left) and inverse (right) hierarchy. HNLs with a mass 1 GeV and only right-handed interactions are considered. Corrections due to the nonzero muon mass are neglected. The absence of τ -coupled interactions enables probing the flavor structure even without observing the initial lepton in the $D^{\pm} \to X l_{\alpha}^{\pm} N$ decay. The colored horizontal band on top shows the dependence on η (bottom axis) for the coherent case, with the range of possible values (upper axis) limited by the blue bands in the colormap. The main plot shows the dependence of the ratio on the parameters η , ϕ_1 for the decoherent case, with the dashed regions depicting the values that lie between the blue band. The coherent case can be excluded for points outside the dashed region. The plots are periodic in η , ϕ_1 .

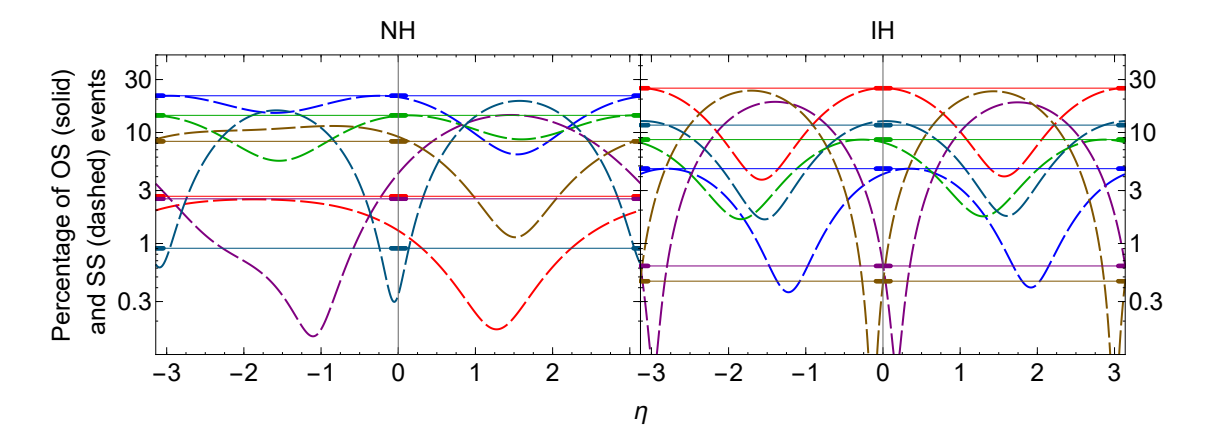


Figure 7. The relative fractions of the opposite-sign (OS, solid lines) and same-sign (SS, dashed lines) events for various combinations of lepton flavors in the final state and the normal (left) or inverse (right) neutrino mass hierarchy. For some values of the Majorana phase η , a conspicuous feature in the signal is a higher rate of lepton number violating events compared to lepton number conserving events. The feature is most prominent in the $\mu\tau$, $e\mu$ channel for NH, and the $e\mu$, $e\tau$ channels for IH.

 Z_R -boson of the extended gauge group, and the breakdown of the symmetry between the left- U_L and right-handed U_R couplings. For example, the HNL production cross-section for the left [121] and right-handed interactions [113] have the following scalings:

$$\sigma^L \sim \frac{U_L^2}{m_W^2}, \qquad \qquad \sigma^R(s < m_{W_R}^2) \sim \frac{s}{m_{W_R}^4} \sim U_R^4 \frac{s}{m_{W_R}^4}$$

where the center-of-mass energy \sqrt{s} is conservatively assumed to be below the W_R mass. It might be possible that, for some parameter space in which $U_R > U_L$, the LH-production dominates the RH one for the parameter space.

The main process for HNLs with RH-interactions is a pair production and decay $l^+l^- \rightarrow N_I N_J \rightarrow (l_1 X)(l_2 Y)$. The flavor and charge composition of the final leptons provides a window into the properties of HNLs. In comparison with the previous setups, the initial lepton flavor and charge are fixed, and two HNLs are present, making the relation of experimental measurements to the couplings V^R more convoluted. The same/opposite sign signature, which refers to the charges of $l_1 l_2$, still serves as a powerful probe of nontrivial dynamics in the HNL sector. The opposite-sign events occur through double LNV or double LNC decays of the two N, while the same-sign events require one LNV and one LNC decay. Deviation of the SS/OS ratios from the trivial unit (Majorana/decoherent case) or zero (approximate symmetry) values would be an indication of the coherent pair. The exact procedure for computing these ratios for the coherent case has to account for two interferences: one coming from the production of HNLs and one coming from their decays as a single tied state. The schematic formula for the amplitude is:

$$\begin{split} \langle l_{\beta}^{+} l_{\gamma}^{\pm} | (NN\text{-mediated}) | l_{\alpha}^{+} l_{\alpha}^{-} \rangle \\ &\Longrightarrow \sum_{IJ} \langle l_{\beta}^{+} l_{\gamma}^{\pm} | (\text{decay}) | N_{I} N_{J} \rangle (C_{W} V_{\alpha I} V_{\alpha J}^{*} + C_{W} V_{\alpha I}^{*} V_{\alpha J} + C_{Z} \delta_{IJ}) \\ &\Longrightarrow \sum_{IJ} (\tilde{C}_{W} V_{\beta I} V_{\gamma J}^{(*)} + \tilde{C}_{W} V_{\gamma I}^{(*)} V_{\beta J}) (C_{W} V_{\alpha I} V_{\alpha J}^{*} + C_{W} V_{\alpha I}^{*} V_{\alpha J} + C_{Z} \delta_{IJ}) \end{split}$$

where C_W , and C_Z are kinematic factors for production through the charged and neutral current, respectively, and \tilde{C}_W is the kinematic factor for HNL decay. These factors are independent of the lepton flavor by construction, once charge lepton masses are neglected. The notation $V^{(*)}$ refers to V for the l_{γ}^+ and V^* for the l_{γ}^- choice. For a given model, the kinematic factors can be computed explicitly and substituted into the formula to give the probability of various combinations of final lepton states.

4.3 Dark matter at SHiP

This section aims to estimate the potential of the SHiP experiment to measure non-minimal interactions of HNLs and ultimately probe the DM candidate N_1 . The SHiP experiment offers an excellent sensitivity to long-living HNLs in both the minimal scenario [8] and the LRSM [125]. For the dark matter searches, the situation is different: since the search for decays of virtually stable DM particles is impossible, the conventional approach [126] relies on the scattering of new physics in the Scattering and Neutrino Detector, and has limited potential in searches for the sterile neutrino. The reason is that N_1 interacts even more weakly than the active neutrino, for which less than 10^7 events are expected [127]. In addition, events with active neutrinos constitute a background for the new physics search, further suppressing the sensitivity. In the minimal case of left-handed interactions, the search for DM in the decays of long-living HNLs is not feasible as well: the amplitude of the decay into the light DM is suppressed by the square of the small mixing angle, one for every new species. In contrast, the right-handed interactions do not have such a problem, for the equivalent small coupling originates from the propagator of the heavy W_R , which suppresses the probability only once.

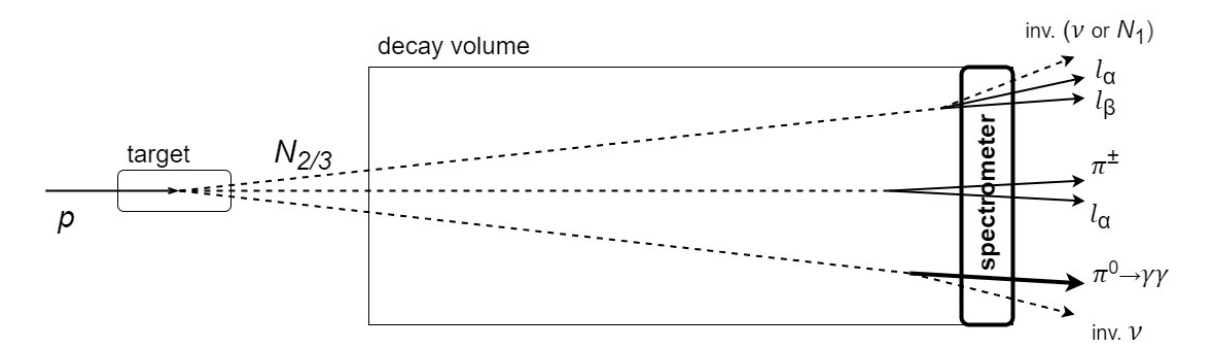


Figure 8. Schematic depiction of new physics detection at SHiP. HNLs are produced in proton-nucleus collisions in the target, move into the decay volume, and decay via one of the three main decay channels: leptonic $l\bar{l}$ +invisible neutrino or light N_1 , lCC into a charged lepton and hadrons, and NC into hadrons with total charge zero plus invisible neutrino.

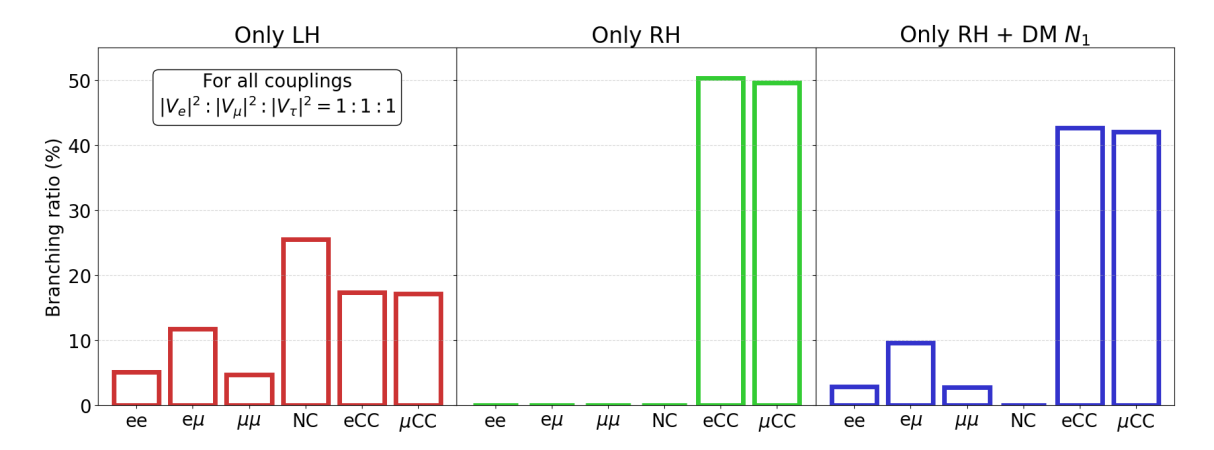


Figure 9. Branching ratios for different theoretical setups: dominant left-handed interactions (left), right-handed interactions (middle), and right-handed interaction with light N_1 (right).

The analysis is based on the branching ratios of visible decay modes, following the methodology of [49, 50]. The main idea is the following: N_1 is expected to be much lighter than the detectable HNL pair $N_{2/3}$ and would give rise to the decay:

$$N_{2/3} \to l_{\alpha} \bar{l}_{\beta} + \text{invisible}$$

which mimics a similar process with a neutrino. The way this decay adjusts the observed branching ratios is, however, non-trivial. The overall scheme of the experiment is shown in figure 8 with the decay modes of interest: $l\bar{l}$, lCC (charged lepton and hadrons) and NC (neutrino and neutral hadrons). The lCC mode provides a precise measurement of the HNL mass. Simpler models without a light N_1 , such as the commonly accepted phenomenology of HNL with left-handed interactions, would be insufficient and fail to fit the observed set of final states.

Three basic scenarios serving as starting points are: LH-dominated case, RH-dominated case, and RH-dominated with a light N_1 species. The qualitative picture highlighting the differences between the three cases is shown in figure 9. The main feature of both RH cases is the absence of the NC mode. Furthermore, HNLs without the N_1 decay only semileptonically

into lCC, making this case the most easily identifiable. The LH and RH+ N_1 are more difficult to distinguish since both have the $l_{\alpha}l_{\beta}$ mode. To establish the difference, one has to rely on the NC mode, as well as on the relative ratios between $l\bar{l}$ and lCC. These three scenarios can readily be distinguished with as few as tens of events.

Any observed experimental result must be tested and compared to all possible theoretical scenarios, including the case of left and right-handed interaction strengths being of the same order. The main result of this section is a demonstration that the DM candidate can still be probed in this scenario with a sufficiently high amount of statistics. For the demonstration, we adopt the following benchmark model: the HNLs have the mass of 1.5 GeV, decay decoherently, and have the couplings:

$$\begin{split} |V_e^L|^2:|V_\mu^L|^2:|V_\tau^L|^2 &= 0.11:0.22:0.67\\ |V_{e2}^R|^2:|V_{\mu2}^R|^2:|V_{\tau2}^R|^2 &= 0.16:0.46:0.38\\ |V_{e3}^R|^2:|V_{\mu3}^R|^2:|V_{\tau3}^R|^2 &= 0.16:0.46:0.38\\ |V_{e1}^R|^2:|V_{\mu3}^R|^2:|V_{\tau3}^R|^2 &= 0.49:0.22:0.30\\ \mathcal{R} &\equiv \frac{U_R^2}{U_L^2+U_R^2} \end{split}$$

chosen to be equal for N_2 and N_3 , and consistent with the parameter space of type-I seesaw of section 3.2 (normal hierarchy). The parameter \mathcal{R} is a free parameter that quantifies the contribution of RH interactions.

For a given $\mathcal{R} < 1$, we want to distinguish

- 1. the benchmark model without the light N_1 versus a single LH-interacting HNL with arbitrary couplings V^L ,
- 2. the benchmark model with the light N_1 versus a single LH-interacting HNL with arbitrary couplings V^L ,
- 3. the benchmark model with the light N_1 versus a single HNL with both left and right interactions and arbitrary couplings V^L , V^R , and \mathcal{R} , but without N_1 .

We compute the branching ratios for each case and use the package from [49] to estimate the required number of events. To recapitulate, the package estimates the number of events that the real model should predict, which would suffice to reject a tested model at a 90% confidence level in at least 90% of experiment realizations (given the probabilistic nature of any experimental result). We assume the most optimistic scenario of zero background and equal detection efficiency for all decay channels. The results are shown in figure 10. For the dominant RH case $\mathcal{R}=1$ and an existing light DM candidate, less than a hundred events might be enough to exclude an HNL with arbitrary left and right couplings but no DM. These estimates should be treated as general lower limits and must be corrected in the proper analysis to account for the actual limitations of the detector systems: particle misidentification, different reconstruction efficiencies, and theoretical uncertainties in the branching ratios, such as those arising from the imprecise HNL mass measurement.

It must be stressed that the third case is the most general test, assuming an HNL with arbitrary left and right couplings. In this sense, the data analysis does not have to rely in

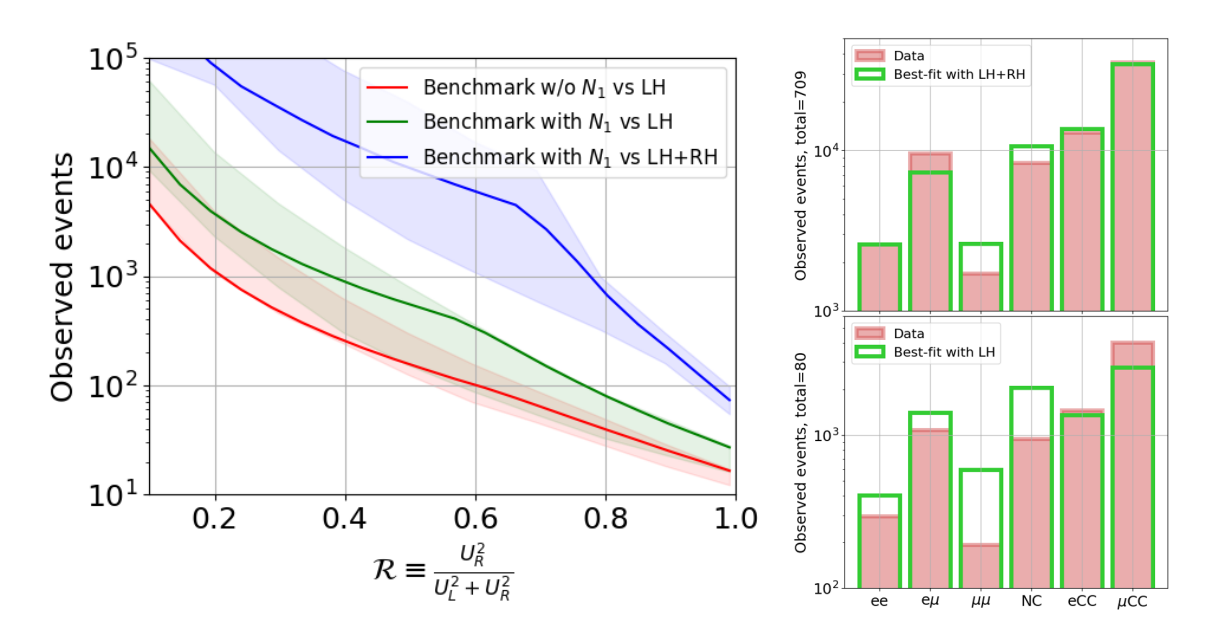


Figure 10. Left: number of observed events in the benchmark model, needed to exclude the tested model versus the benchmark model at 90% confidence level with 90% probability. The solid lines correspond to the differentiation between the benchmark models and the tested models. The filled regions represent the variation of the results for some randomly picked combinations of couplings, consistent with figure 3, in place of the benchmark model. Right: an illustration of the branching ratios for the benchmark model with a DM candidate and their incompatibility with LH+RH (top) and LH (bottom) models.

any way on the approximate symmetry limit setup. Therefore, the conclusions about the possibility of probing the light candidate are not restricted to our specific model. The same analysis can be performed for an arbitrary set of couplings of the light and heavier species; the inconsistency of the signal with the model without N_1 will be more or less pronounced but still present, except for some fine-tuned cases, such as complete DM-tau lepton coupling, $|V_{1\tau}^R| = 1$.

In the case of the discovery of new physics, the observation may indicate some kind of non-minimality that requires combined left and right interactions. This would correspond to the region above the green line of figure 10. In such a scenario, it would be imperative to investigate further whether the signal contains a contribution of N_1 decays. The blue line quantifies the minimal required sensitivity of a follow-up experiment, needed to have a decisive answer. This estimate depends on the unknown underlying theory; however, one can obtain a general reference point: in the case of a slight deviation (say, 2σ) of the observation from the pure LH model, the number of required events should increase by roughly an order of magnitude.

5 Conclusions

In this work, we have investigated the attractive scenario of a quasi-degenerate pair of Heavy Neutral Leptons within the Left-Right Symmetric Model. A degenerate pair can facilitate the generation of baryon asymmetry and, at the same time, be within the reach of future experimental searches without leading to too large masses of active neutrinos. Compared to the minimal case, the HNLs in the Left-Right Symmetric Model possess additional interactions through the right-handed current, which have new phenomenological implications.

We analyzed the flavor structure of the right-handed HNL couplings from the full seesaw relation in the approximate symmetry limit. A notable result is the concrete predictions for effective right-handed couplings. These predictions serve as tangible targets for experimental tests of the model.

Moreover, we explored the potential impact of our findings on various experimental probes in the considered model. Our assessment of the sensitivity of FCC-ee to detect HNLs in the combined model, along with the provision of simple scaling arguments, shows that right-handed interactions can improve the sensitivity to the left-handed couplings. We examined the properties of the quasi-degenerate HNL pair in the coherent and decoherent cases, which offer different rich phenomenology. We discussed the experimental signatures that can be employed for SHiP, FCC-ee, and future hadron and lepton colliders.

Finally, we demonstrated for the first time the potential of the recently approved SHiP experiment to probe the existence of the dark matter candidate in decays of HNLs. Our analysis suggests that, in the best-case scenario, SHiP could provide compelling evidence for dark matter with fewer than a hundred events. Our findings were enabled by extending the new physics model to include possible nonminimal interactions, while striving to retain its predictive power. This highlights the necessity for further research to explore the full potential of next-generation experiments.

Acknowledgments

I thank Kevin Alberto Urquía Calderón, Marco Drewes, Miha Nemevšek, and Alexey Boyarsky for their comments and suggestions. This project has received funding from the European Research Council (ERC) under the European Union's Horizon 2020 research and innovation programme (GA 694896), from the NWO Physics Vrij Programme "The Hidden Universe of Weakly Interacting Particles", No. 680.92.18.03, which is partly financed by the Dutch Research Council NWO. Feynman diagrams have been computed with the use of FeynCalc [128].

A Decay $N_I \rightarrow N_I l_{\alpha} l_{\beta}$

The decay width is given by

$$\Gamma(N_I \to N_J l_\alpha \bar{l}_\beta) = U_R^2 \frac{G_F^2 m_{N_I}^5}{16\pi^2} \int_{(x_\alpha + x_\beta)^2}^{(1 - x_J)^2} \frac{dx}{x} \sqrt{\lambda(1, x, x_J^2) \lambda(x, x_\alpha^2, x_\beta^2)} (x - x_\alpha^2 - x_\beta^2)$$

$$\left((1 + x_J^2 - x)(|V_{\alpha I}^R|^2 |V_{\beta J}^R|^2 + |V_{\beta I}^R|^2 |V_{\alpha J}^R|^2) - 2x_J \text{Re}[V_{\alpha I}^R V_{\alpha J}^R V_{\beta I}^{*R} V_{\beta J}^{*R}] \right).$$

Here, $x_J=m_{N_J}/m_{N_I},\; x_{\alpha}=m_{l_{\alpha}}/m_{N_I},\; x_{\beta}=m_{l_{\beta}}/m_{N_I},\; {\rm and}\;$

$$\lambda(a, b, c) = a^{2} + b^{2} + c^{2} - 2ab - 2ac - 2bc$$

B Parametrization of the seesaw relation

The parameters entering eq. (3.14) are related to the initial perturbation parameters defined in eq. (3.12) as:

$$\epsilon_1 = \Delta_{21} + i\Delta_{31} \tag{B.1}$$

$$\epsilon_2 = \Delta_{22} + \Delta_{33} - i(\Delta_{23} - \Delta_{32}) + \kappa$$
 (B.2)

$$\epsilon_3 = \Delta_{22} - \Delta_{33} + i(\Delta_{23} + \Delta_{32}) - \mu$$
 (B.3)

To get the parametric solution in the form of eq. (3.17), these parameters should be equal to

$$\epsilon_1 = \xi \times \frac{1}{\sqrt{2}} e^{i(\phi_0 + \phi_2)} s_{2\gamma} s_{\psi} \tag{B.4}$$

$$\epsilon_2 = \xi \times e^{i\phi_0} s_{2\gamma} c_{\psi} \tag{B.5}$$

$$\epsilon_3 = \xi \times e^{i(\phi_0 + \phi_1)} c_{2\gamma} \tag{B.6}$$

$$\xi = \frac{m_2 + m_3}{m_N U_L^2} \tag{B.7}$$

The matrix $\Delta = \Delta^H + \Delta^A$ can be split into a hermitian $\Delta^H = \Delta^{H\dagger}$ and anti-hermitian $\Delta^A = -\Delta^{A\dagger}$ parts. The conditions above can be fully absorbed into the hermitian part, allowing the anti-hermitian part to be largely arbitrary:

$$\epsilon_{1}: \qquad \Delta_{21}^{H} + i\Delta_{31}^{H} = \frac{\xi}{\sqrt{2}} e^{i(\psi_{0} + \psi_{2})} s_{2\gamma} s_{\psi} - \Delta_{21}^{A} - i\Delta_{31}^{A}$$

$$\epsilon_{3}: \Delta_{22}^{H} - \Delta_{33}^{H} + 2i \operatorname{Re} \Delta_{23}^{H} = \xi e^{i(\phi_{0} + \psi_{1})} c_{2\gamma} - \Delta_{22}^{A} + \Delta_{33}^{A} + 2\operatorname{Im} \Delta_{23}^{A}$$

which are straightforward to satisfy by adjusting Δ^H . The third equation related to ϵ_2 requires more care:

$$\epsilon_2: \Delta_{22}^H + \Delta_{33}^H + 2\operatorname{Im}\Delta_{23}^H = \xi e^{i\phi_0} s_{2\gamma} c_{\psi} - \Delta_{22}^A - \Delta_{33}^A + 2i\operatorname{Re}\Delta_{23}^A$$
 (B.8)

where the l.h.s. of the last equation is always real. This means that the imaginary part of r.h.s. should vanish, which removes one degree of freedom and fixes ϕ_0 for a given Δ^A :

$$\xi s_{2\gamma} c_{\psi} \sin \phi_0 = \text{Im}(\Delta_{22}^A + \Delta_{33}^A) + 2\text{Re}\Delta_{23}^A$$
 (B.9)

The mixing angle of the DM candidate satisfies:

$$\left(\frac{m_{N_1}U_1^L}{m_N U_L}\right)^2 = \frac{|\Delta_{11}|^2 + |\Delta_{12}|^2 + |\Delta_{13}|^2}{2} \tag{B.10}$$

Using the relation $(\Delta_{12} - i\Delta_{13})^* = \epsilon_1 - 2\Delta_{21}^A - 2i\Delta_{31}^A$, the inequality

$$|\Delta_{12}|^2 + |\Delta_{13}|^2 \ge \frac{|\Delta_{12} - i\Delta_{13}|^2}{2}$$

and the parametrization (B.4), we obtain

$$\left(\frac{m_{N_1}U_1^L}{m_N U_L}\right)^2 \ge \frac{|\Delta_{11}|^2}{2} + \left|\frac{\xi}{2\sqrt{2}}e^{i(\phi_0 + \phi_2)}s_{2\gamma}c_{\psi} - \Delta_{21}^A - i\Delta_{31}^A\right|^2$$
(B.11)

Data Availability Statement. This article has no associated data or the data will not be deposited.

Code Availability Statement. This article has no associated code or the code will not be deposited.

Open Access. This article is distributed under the terms of the Creative Commons Attribution License (CC-BY4.0), which permits any use, distribution and reproduction in any medium, provided the original author(s) and source are credited.

References

- [1] P. Minkowski, $\mu \to e \gamma$ at a Rate of One Out of 10⁹ Muon Decays?, Phys. Lett. B **67** (1977) 421 [INSPIRE].
- [2] R.N. Mohapatra and G. Senjanovic, Neutrino Mass and Spontaneous Parity Nonconservation, Phys. Rev. Lett. 44 (1980) 912 [INSPIRE].
- [3] R.N. Mohapatra and G. Senjanovic, Neutrino Masses and Mixings in Gauge Models with Spontaneous Parity Violation, Phys. Rev. D 23 (1981) 165 [INSPIRE].
- [4] J. Schechter and J.W.F. Valle, Neutrino Masses in $SU(2) \times U(1)$ Theories, Phys. Rev. D 22 (1980) 2227 [INSPIRE].
- [5] R.N. Mohapatra et al., Theory of neutrinos: A White paper, Rept. Prog. Phys. 70 (2007) 1757 [hep-ph/0510213] [INSPIRE].
- [6] A.M. Abdullahi et al., The present and future status of heavy neutral leptons, J. Phys. G 50 (2023) 020501 [arXiv:2203.08039] [INSPIRE].
- [7] SHIP collaboration, A facility to Search for Hidden Particles (SHiP) at the CERN SPS, arXiv:1504.04956 [INSPIRE].
- [8] SHIP collaboration, Sensitivity of the SHiP experiment to Heavy Neutral Leptons, JHEP 04 (2019) 077 [arXiv:1811.00930] [INSPIRE].
- [9] DUNE collaboration, Long-Baseline Neutrino Facility (LBNF) and Deep Underground Neutrino Experiment (DUNE): Conceptual Design Report, Volume 2: The Physics Program for DUNE at LBNF, arXiv:1512.06148 [INSPIRE].
- [10] P. Ballett, T. Boschi and S. Pascoli, Heavy Neutral Leptons from low-scale seesaws at the DUNE Near Detector, JHEP 03 (2020) 111 [arXiv:1905.00284] [INSPIRE].
- [11] I. Krasnov, DUNE prospects in the search for sterile neutrinos, Phys. Rev. D 100 (2019) 075023 [arXiv:1902.06099] [INSPIRE].
- [12] F. Kling and S. Trojanowski, Heavy Neutral Leptons at FASER, Phys. Rev. D 97 (2018) 095016 [arXiv:1801.08947] [INSPIRE].
- [13] A. Boyarsky, O. Mikulenko, M. Ovchynnikov and L. Shchutska, Searches for new physics at SND@LHC, JHEP 03 (2022) 006 [arXiv:2104.09688] [INSPIRE].
- [14] D. Curtin et al., Long-Lived Particles at the Energy Frontier: The MATHUSLA Physics Case, Rept. Prog. Phys. 82 (2019) 116201 [arXiv:1806.07396] [INSPIRE].
- [15] D. Dercks, H.K. Dreiner, M. Hirsch and Z.S. Wang, Long-Lived Fermions at AL3X, Phys. Rev. D 99 (2019) 055020 [arXiv:1811.01995] [INSPIRE].

- [16] M. Hirsch and Z.S. Wang, Heavy neutral leptons at ANUBIS, Phys. Rev. D 101 (2020) 055034 [arXiv:2001.04750] [INSPIRE].
- [17] CODEX-B collaboration, Expression of interest for the CODEX-b detector, Eur. Phys. J. C 80 (2020) 1177 [arXiv:1911.00481] [INSPIRE].
- [18] J.L. Feng et al., The Forward Physics Facility at the High-Luminosity LHC, J. Phys. G 50 (2023) 030501 [arXiv:2203.05090] [INSPIRE].
- [19] M. Ovchynnikov, V. Kryshtal and K. Bondarenko, Sensitivity of the FACET experiment to Heavy Neutral Leptons and Dark Scalars, JHEP 02 (2023) 056 [arXiv:2209.14870] [INSPIRE].
- [20] S. Antusch, E. Cazzato and O. Fischer, Sterile neutrino searches at future e^-e^+ , pp, and e^-p colliders, Int. J. Mod. Phys. A 32 (2017) 1750078 [arXiv:1612.02728] [INSPIRE].
- [21] A. Blondel et al., Searches for long-lived particles at the future FCC-ee, Front. in Phys. 10 (2022) 967881 [arXiv:2203.05502] [INSPIRE].
- [22] M. Chrząszcz, M. Drewes and J. Hajer, *HECATE: A long-lived particle detector concept for the FCC-ee or CEPC, Eur. Phys. J. C* 81 (2021) 546 [arXiv:2011.01005] [INSPIRE].
- [23] K. Mękała, J. Reuter and A.F. Żarnecki, *Heavy neutrinos at future linear* e^+e^- *colliders*, *JHEP* **06** (2022) 010 [arXiv:2202.06703] [INSPIRE].
- [24] A. Boyarsky, O. Mikulenko, M. Ovchynnikov and L. Shchutska, Exploring the potential of FCC-hh to search for particles from B mesons, JHEP **01** (2023) 042 [arXiv:2204.01622] [INSPIRE].
- [25] P. Li, Z. Liu and K.-F. Lyu, Heavy neutral leptons at muon colliders, JHEP 03 (2023) 231 [arXiv:2301.07117] [INSPIRE].
- [26] T.H. Kwok, L. Li, T. Liu and A. Rock, Searching for heavy neutral leptons at a future muon collider, Phys. Rev. D 110 (2024) 075009 [arXiv:2301.05177] [INSPIRE].
- [27] A.D. Dolgov, S.H. Hansen, G. Raffelt and D.V. Semikoz, Heavy sterile neutrinos: Bounds from big bang nucleosynthesis and SN1987A, Nucl. Phys. B 590 (2000) 562 [hep-ph/0008138] [INSPIRE].
- [28] N. Sabti, A. Magalich and A. Filimonova, An Extended Analysis of Heavy Neutral Leptons during Big Bang Nucleosynthesis, JCAP 11 (2020) 056 [arXiv:2006.07387] [INSPIRE].
- [29] A. Boyarsky, M. Ovchynnikov, O. Ruchayskiy and V. Syvolap, *Improved big bang nucleosynthesis constraints on heavy neutral leptons*, *Phys. Rev. D* **104** (2021) 023517 [arXiv:2008.00749] [INSPIRE].
- [30] A.C. Vincent et al., Revisiting cosmological bounds on sterile neutrinos, JCAP 04 (2015) 006 [arXiv:1408.1956] [INSPIRE].
- [31] V. Poulin, J. Lesgourgues and P.D. Serpico, Cosmological constraints on exotic injection of electromagnetic energy, JCAP 03 (2017) 043 [arXiv:1610.10051] [INSPIRE].
- [32] V. Syvolap, O. Ruchayskiy and A. Boyarsky, Resonance production of keV sterile neutrinos in core-collapse supernovae and lepton number diffusion, Phys. Rev. D 106 (2022) 015017 [arXiv:1909.06320] [INSPIRE].
- [33] T. Rembiasz et al., Heavy sterile neutrinos in stellar core-collapse, Phys. Rev. D 98 (2018) 103010 [arXiv:1806.03300] [INSPIRE].
- [34] A.M. Suliga, I. Tamborra and M.-R. Wu, Tau lepton asymmetry by sterile neutrino emission Moving beyond one-zone supernova models, JCAP 12 (2019) 019 [arXiv:1908.11382] [INSPIRE].

- [35] A. Ray and Y.-Z. Qian, Evolution of tau-neutrino lepton number in protoneutron stars due to active-sterile neutrino mixing, Phys. Rev. D 108 (2023) 063025 [arXiv:2306.08209] [INSPIRE].
- [36] A. Ray and Y.-Z. Qian, Enhanced muonization by active-sterile neutrino mixing in protoneutron stars, Phys. Rev. D 110 (2024) 043007 [arXiv:2404.14485] [INSPIRE].
- [37] P. Coloma, P.A.N. Machado, I. Martinez-Soler and I.M. Shoemaker, *Double-Cascade Events from New Physics in Icecube*, *Phys. Rev. Lett.* **119** (2017) 201804 [arXiv:1707.08573] [INSPIRE].
- [38] R.A. Gustafson, R. Plestid and I.M. Shoemaker, Neutrino portals, terrestrial upscattering, and atmospheric neutrinos, Phys. Rev. D 106 (2022) 095037 [arXiv:2205.02234] [INSPIRE].
- [39] ICECUBE collaboration, Search for Heavy Neutral Lepton Production and Decay with the IceCube Neutrino Observatory, PoS ICHEP2022 (2022) 190 [INSPIRE].
- [40] S. Antusch and O. Fischer, Non-unitarity of the leptonic mixing matrix: Present bounds and future sensitivities, JHEP 10 (2014) 094 [arXiv:1407.6607] [INSPIRE].
- [41] E. Fernandez-Martinez, J. Hernandez-Garcia and J. Lopez-Pavon, *Global constraints on heavy neutrino mixing*, *JHEP* 08 (2016) 033 [arXiv:1605.08774] [INSPIRE].
- [42] M. Chrzaszcz et al., A frequentist analysis of three right-handed neutrinos with GAMBIT, Eur. Phys. J. C 80 (2020) 569 [arXiv:1908.02302] [INSPIRE].
- [43] M. Drewes and S. Eijima, Neutrinoless double β decay and low scale leptogenesis, Phys. Lett. B 763 (2016) 72 [arXiv:1606.06221] [INSPIRE].
- [44] W. Dekens et al., Sterile neutrinos and neutrinoless double beta decay in effective field theory, JHEP 06 (2020) 097 [arXiv:2002.07182] [INSPIRE].
- [45] J. de Vries et al., Confronting the low-scale seesaw and leptogenesis with neutrinoless double beta decay, JHEP 05 (2025) 090 [arXiv:2407.10560] [INSPIRE].
- [46] R.H. Bernstein and P.S. Cooper, Charged Lepton Flavor Violation: An Experimenter's Guide, Phys. Rept. 532 (2013) 27 [arXiv:1307.5787] [INSPIRE].
- [47] L. Calibbi and G. Signorelli, Charged Lepton Flavour Violation: An Experimental and Theoretical Introduction, Riv. Nuovo Cim. 41 (2018) 71 [arXiv:1709.00294] [INSPIRE].
- [48] K.A. Urquía-Calderón, I. Timiryasov and O. Ruchayskiy, *Heavy neutral leptons Advancing into the PeV domain*, *JHEP* **08** (2023) 167 [arXiv:2206.04540] [INSPIRE].
- [49] O. Mikulenko, K. Bondarenko, A. Boyarsky and O. Ruchayskiy, *Unveiling new physics with discoveries at Intensity Frontier*, arXiv:2312.05163 [INSPIRE].
- [50] O. Mikulenko, K. Bondarenko, A. Boyarsky and O. Ruchayskiy, New physics at the Intensity Frontier: how much can we learn and how?, arXiv:2312.00659 [INSPIRE].
- [51] T. Asaka, S. Blanchet and M. Shaposhnikov, *The nuMSM, dark matter and neutrino masses*, *Phys. Lett. B* **631** (2005) 151 [hep-ph/0503065] [INSPIRE].
- [52] T. Asaka and M. Shaposhnikov, The νMSM, dark matter and baryon asymmetry of the universe, Phys. Lett. B **620** (2005) 17 [hep-ph/0505013] [INSPIRE].
- [53] M. Drewes et al., A White Paper on keV Sterile Neutrino Dark Matter, JCAP 01 (2017) 025 [arXiv:1602.04816] [INSPIRE].
- [54] A. Boyarsky et al., Sterile neutrino Dark Matter, Prog. Part. Nucl. Phys. 104 (2019) 1 [arXiv:1807.07938] [INSPIRE].

- [55] S. Tremaine and J.E. Gunn, Dynamical Role of Light Neutral Leptons in Cosmology, Phys. Rev. Lett. 42 (1979) 407 [INSPIRE].
- [56] A. Boyarsky, O. Ruchayskiy and D. Iakubovskyi, A Lower bound on the mass of Dark Matter particles, JCAP 03 (2009) 005 [arXiv:0808.3902] [INSPIRE].
- [57] K. Abazajian, G.M. Fuller and W.H. Tucker, Direct detection of warm dark matter in the X-ray, Astrophys. J. 562 (2001) 593 [astro-ph/0106002] [INSPIRE].
- [58] J. Kersten and A.Y. Smirnov, Right-Handed Neutrinos at CERN LHC and the Mechanism of Neutrino Mass Generation, Phys. Rev. D 76 (2007) 073005 [arXiv:0705.3221] [INSPIRE].
- [59] E.K. Akhmedov, V.A. Rubakov and A.Y. Smirnov, *Baryogenesis via neutrino oscillations*, *Phys. Rev. Lett.* **81** (1998) 1359 [hep-ph/9803255] [INSPIRE].
- [60] L. Canetti and M. Shaposhnikov, Baryon Asymmetry of the Universe in the NuMSM, JCAP 09 (2010) 001 [arXiv:1006.0133] [INSPIRE].
- [61] L. Canetti, M. Drewes and M. Shaposhnikov, Sterile Neutrinos as the Origin of Dark and Baryonic Matter, Phys. Rev. Lett. 110 (2013) 061801 [arXiv:1204.3902] [INSPIRE].
- [62] J. Klarić, M. Shaposhnikov and I. Timiryasov, Uniting Low-Scale Leptogenesis Mechanisms, Phys. Rev. Lett. 127 (2021) 111802 [arXiv:2008.13771] [INSPIRE].
- [63] J. Klarić, M. Shaposhnikov and I. Timiryasov, Reconciling resonant leptogenesis and baryogenesis via neutrino oscillations, Phys. Rev. D 104 (2021) 055010 [arXiv:2103.16545] [INSPIRE].
- [64] M. Fukugita and T. Yanagida, Baryogenesis Without Grand Unification, Phys. Lett. B 174 (1986) 45 [INSPIRE].
- [65] S. Davidson, E. Nardi and Y. Nir, Leptogenesis, Phys. Rept. 466 (2008) 105 [arXiv:0802.2962] [INSPIRE].
- [66] G. Magill, R. Plestid, M. Pospelov and Y.-D. Tsai, Dipole Portal to Heavy Neutral Leptons, Phys. Rev. D 98 (2018) 115015 [arXiv:1803.03262] [INSPIRE].
- [67] M. Ovchynnikov and J.-Y. Zhu, Search for the dipole portal of heavy neutral leptons at future colliders, JHEP 07 (2023) 039 [arXiv:2301.08592] [INSPIRE].
- [68] M. Ovchynnikov, T. Schwetz and J.-Y. Zhu, Dipole portal and neutrinophilic scalars at DUNE revisited: The importance of the high-energy neutrino tail, Phys. Rev. D 107 (2023) 055029 [arXiv:2210.13141] [INSPIRE].
- [69] A. de Giorgi, L. Merlo and J.-L. Tastet, Probing HNL-ALP couplings at colliders, Fortsch. Phys. 71 (2023) 2300027 [arXiv:2212.11290] [INSPIRE].
- [70] A.M. Abdullahi et al., Heavy Neutral Leptons via Axionlike Particles at Neutrino Facilities, Phys. Rev. Lett. 133 (2024) 261802 [arXiv:2311.07713] [INSPIRE].
- [71] E. Fernández-Martínez et al., Effective portals to heavy neutral leptons, JHEP **09** (2023) 001 [arXiv:2304.06772] [INSPIRE].
- [72] J.C. Pati and A. Salam, Lepton Number as the Fourth Color, Phys. Rev. D 10 (1974) 275 [INSPIRE].
- [73] CMS collaboration, Search for high-mass resonances in final states with a lepton and missing transverse momentum at $\sqrt{s} = 13$ TeV, JHEP **06** (2018) 128 [arXiv:1803.11133] [INSPIRE].

- [74] ATLAS collaboration, Search for a heavy charged boson in events with a charged lepton and missing transverse momentum from pp collisions at $\sqrt{s} = 13$ TeV with the ATLAS detector, Phys. Rev. D 100 (2019) 052013 [arXiv:1906.05609] [INSPIRE].
- [75] CMS collaboration, Search for a right-handed W boson and a heavy neutrino in proton-proton collisions at $\sqrt{s} = 13$ TeV, JHEP **04** (2022) 047 [arXiv:2112.03949] [INSPIRE].
- [76] ATLAS collaboration, Search for heavy Majorana or Dirac neutrinos and right-handed W gauge bosons in final states with charged leptons and jets in pp collisions at $\sqrt{s} = 13$ TeV with the ATLAS detector, Eur. Phys. J. C 83 (2023) 1164 [arXiv:2304.09553] [INSPIRE].
- [77] G. Cottin, J.C. Helo, M. Hirsch and D. Silva, Revisiting the LHC reach in the displaced region of the minimal left-right symmetric model, Phys. Rev. D 99 (2019) 115013 [arXiv:1902.05673] [INSPIRE].
- [78] S. Bertolini, A. Maiezza and F. Nesti, Present and Future K and B Meson Mixing Constraints on TeV Scale Left-Right Symmetry, Phys. Rev. D 89 (2014) 095028 [arXiv:1403.7112] [INSPIRE].
- [79] G.F.S. Alves, C.S. Fong, L.P.S. Leal and R. Zukanovich Funchal, Limits on WR from Meson Decays, Phys. Rev. Lett. 133 (2024) 161802 [arXiv:2307.04862] [INSPIRE].
- [80] V. Tello et al., Left-Right Symmetry: from LHC to Neutrinoless Double Beta Decay, Phys. Rev. Lett. 106 (2011) 151801 [arXiv:1011.3522] [INSPIRE].
- [81] J. Gluza, T. Jelinski and R. Szafron, Lepton number violation and 'Diracness' of massive neutrinos composed of Majorana states, Phys. Rev. D 93 (2016) 113017 [arXiv:1604.01388] [INSPIRE].
- [82] J. de Vries et al., Probing light sterile neutrinos in left-right symmetric models with displaced vertices and neutrinoless double beta decay, JHEP **04** (2025) 007 [arXiv:2406.15091] [INSPIRE].
- [83] J.-M. Frere, T. Hambye and G. Vertongen, *Is leptogenesis falsifiable at LHC?*, *JHEP* **01** (2009) 051 [arXiv:0806.0841] [INSPIRE].
- [84] F. Bezrukov, A. Kartavtsev and M. Lindner, Leptogenesis in models with keV sterile neutrino dark matter, J. Phys. G 40 (2013) 095202 [arXiv:1204.5477] [INSPIRE].
- [85] P.S. Bhupal Dev, C.-H. Lee and R.N. Mohapatra, Leptogenesis Constraints on the Mass of Right-handed Gauge Bosons, Phys. Rev. D 90 (2014) 095012 [arXiv:1408.2820] [INSPIRE].
- [86] M. Dhuria, C. Hati, R. Rangarajan and U. Sarkar, Falsifying leptogenesis for a TeV scale W_R^{\pm} at the LHC, Phys. Rev. D 92 (2015) 031701 [arXiv:1503.07198] [INSPIRE].
- [87] F. Bezrukov, H. Hettmansperger and M. Lindner, keV sterile neutrino Dark Matter in gauge extensions of the Standard Model, Phys. Rev. D 81 (2010) 085032 [arXiv:0912.4415] [INSPIRE].
- [88] M. Nemevsek, G. Senjanovic and Y. Zhang, Warm Dark Matter in Low Scale Left-Right Theory, JCAP 07 (2012) 006 [arXiv:1205.0844] [INSPIRE].
- [89] D. Borah and A. Dasgupta, Left-right symmetric models with a mixture of keV-TeV dark matter, J. Phys. G 46 (2019) 105004 [arXiv:1710.06170] [INSPIRE].
- [90] M. Nemevšek and Y. Zhang, Dark Matter Dilution Mechanism through the Lens of Large-Scale Structure, Phys. Rev. Lett. 130 (2023) 121002 [arXiv:2206.11293] [INSPIRE].
- [91] M. Nemevšek and Y. Zhang, Anatomy of diluted dark matter in the minimal left-right symmetric model, Phys. Rev. D 109 (2024) 056021 [arXiv:2312.00129] [INSPIRE].

- [92] A. Roitgrund, G. Eilam and S. Bar-Shalom, Implementation of the left-right symmetric model in FeynRules, Comput. Phys. Commun. 203 (2016) 18 [arXiv:1401.3345] [INSPIRE].
- [93] M. Mitra, G. Senjanovic and F. Vissani, Neutrinoless Double Beta Decay and Heavy Sterile Neutrinos, Nucl. Phys. B 856 (2012) 26 [arXiv:1108.0004] [INSPIRE].
- [94] C.-Y. Chen, P.S.B. Dev and R.N. Mohapatra, Probing Heavy-Light Neutrino Mixing in Left-Right Seesaw Models at the LHC, Phys. Rev. D 88 (2013) 033014 [arXiv:1306.2342] [INSPIRE].
- [95] G. Senjanović and V. Tello, Restoration of Parity and the Right-Handed Analog of the CKM Matrix, Phys. Rev. D 94 (2016) 095023 [arXiv:1502.05704] [INSPIRE].
- [96] K. Bondarenko, A. Boyarsky, D. Gorbunov and O. Ruchayskiy, *Phenomenology of GeV-scale Heavy Neutral Leptons*, *JHEP* 11 (2018) 032 [arXiv:1805.08567] [INSPIRE].
- [97] W.-Y. Keung and G. Senjanovic, Majorana Neutrinos and the Production of the Right-handed Charged Gauge Boson, Phys. Rev. Lett. **50** (1983) 1427 [INSPIRE].
- [98] G. Senjanović and V. Tello, *Probing Seesaw with Parity Restoration*, *Phys. Rev. Lett.* **119** (2017) 201803 [arXiv:1612.05503] [INSPIRE].
- [99] J.A. Casas and A. Ibarra, Oscillating neutrinos and $\mu \to e, \gamma$, Nucl. Phys. B **618** (2001) 171 [hep-ph/0103065] [INSPIRE].
- [100] M. Nemevsek, G. Senjanovic and V. Tello, Connecting Dirac and Majorana Neutrino Mass Matrices in the Minimal Left-Right Symmetric Model, Phys. Rev. Lett. 110 (2013) 151802 [arXiv:1211.2837] [INSPIRE].
- [101] G. Senjanovic and V. Tello, Disentangling the seesaw mechanism in the minimal left-right symmetric model, Phys. Rev. D 100 (2019) 115031 [arXiv:1812.03790] [INSPIRE].
- [102] G. Senjanovic and V. Tello, Parity and the origin of neutrino mass, Int. J. Mod. Phys. A 35 (2020) 2050053 [arXiv:1912.13060] [INSPIRE].
- [103] M.C. Gonzalez-Garcia, M. Maltoni, J. Salvado and T. Schwetz, Global fit to three neutrino mixing: critical look at present precision, JHEP 12 (2012) 123 [arXiv:1209.3023] [INSPIRE].
- [104] G. Senjanovic, Spontaneous Breakdown of Parity in a Class of Gauge Theories, Nucl. Phys. B 153 (1979) 334 [INSPIRE].
- [105] S.R. Mishra et al., Search for right-handed coupling in neutrino N scattering, Phys. Rev. Lett. 68 (1992) 3499 [INSPIRE].
- [106] TWIST collaboration, Precise measurement of parity violation in polarized muon decay, Phys. Rev. D 84 (2011) 032005 [arXiv:1104.3632] [INSPIRE].
- [107] A. Maiezza, M. Nemevsek, F. Nesti and G. Senjanovic, Left-Right Symmetry at LHC, Phys. Rev. D 82 (2010) 055022 [arXiv:1005.5160] [INSPIRE].
- [108] G. Senjanović and V. Tello, Right Handed Quark Mixing in Left-Right Symmetric Theory, Phys. Rev. Lett. 114 (2015) 071801 [arXiv:1408.3835] [INSPIRE].
- [109] I. Esteban et al., The fate of hints: updated global analysis of three-flavor neutrino oscillations, JHEP 09 (2020) 178 [arXiv:2007.14792] [INSPIRE].
- [110] FCC-EE STUDY TEAM collaboration, Search for Heavy Right Handed Neutrinos at the FCC-ee, Nucl. Part. Phys. Proc. 273-275 (2016) 1883 [arXiv:1411.5230] [INSPIRE].

- [111] K. Bondarenko, A. Boyarsky, M. Ovchynnikov and O. Ruchayskiy, Sensitivity of the intensity frontier experiments for neutrino and scalar portals: analytic estimates, JHEP 08 (2019) 061 [arXiv:1902.06240] [INSPIRE].
- [112] P. Duka, J. Gluza and M. Zralek, Quantization and renormalization of the manifest left-right symmetric model of electroweak interactions, Annals Phys. 280 (2000) 336 [hep-ph/9910279] [INSPIRE].
- [113] K.A. Urquía-Calderón, Long-lived heavy neutral leptons at lepton colliders as a probe of left-right-symmetric models, Phys. Rev. D 109 (2024) 055002 [arXiv:2310.17406] [INSPIRE].
- [114] J.D. Vergados, H. Ejiri and F. Simkovic, *Theory of Neutrinoless Double Beta Decay*, *Rept. Prog. Phys.* **75** (2012) 106301 [arXiv:1205.0649] [INSPIRE].
- [115] S. Antusch, E. Cazzato and O. Fischer, Resolvable heavy neutrino-antineutrino oscillations at colliders, Mod. Phys. Lett. A 34 (2019) 1950061 [arXiv:1709.03797] [INSPIRE].
- [116] S. Antusch et al., Probing Leptogenesis at Future Colliders, JHEP **09** (2018) 124 [arXiv:1710.03744] [INSPIRE].
- [117] A. Das, P.S.B. Dev and R.N. Mohapatra, Same Sign versus Opposite Sign Dileptons as a Probe of Low Scale Seesaw Mechanisms, Phys. Rev. D 97 (2018) 015018 [arXiv:1709.06553] [INSPIRE].
- [118] M. Drewes, J. Klarić and P. Klose, On lepton number violation in heavy neutrino decays at colliders, JHEP 11 (2019) 032 [arXiv:1907.13034] [INSPIRE].
- [119] J.L. Schubert and O. Ruchayskiy, Neutrinoless double-beta decay at colliders: interference between Majorana states, arXiv:2210.11294 [INSPIRE].
- [120] S. Antusch, J. Hajer and B.M.S. Oliveira, *Heavy neutrino-antineutrino oscillations at the FCC-ee*, *JHEP* **10** (2023) 129 [arXiv:2308.07297] [INSPIRE].
- [121] O. Mikulenko and M. Marinichenko, Measuring lepton number violation in heavy neutral lepton decays at the future muon collider, JHEP 01 (2024) 032 [arXiv:2309.16837] [INSPIRE].
- [122] J.-L. Tastet and I. Timiryasov, Dirac vs. Majorana HNLs (and their oscillations) at SHiP, JHEP 04 (2020) 005 [arXiv:1912.05520] [INSPIRE].
- [123] S. Antusch, J. Hajer and J. Rosskopp, Decoherence effects on lepton number violation from heavy neutrino-antineutrino oscillations, JHEP 11 (2023) 235 [arXiv:2307.06208] [INSPIRE].
- [124] A. Blondel, A. de Gouvêa and B. Kayser, Z-boson decays into Majorana or Dirac heavy neutrinos, Phys. Rev. D 104 (2021) 055027 [arXiv:2105.06576] [INSPIRE].
- [125] O. Castillo-Felisola et al., Left-Right Symmetric Models at the High-Intensity Frontier, Phys. Rev. D 92 (2015) 013001 [arXiv:1504.02489] [INSPIRE].
- [126] SHIP collaboration, Sensitivity of the SHiP experiment to light dark matter, JHEP **04** (2021) 199 [arXiv:2010.11057] [INSPIRE].
- [127] SHIP collaboration, Neutrino physics with the SHiP experiment at CERN, J. Phys. Conf. Ser. 1690 (2020) 012171 [INSPIRE].
- [128] V. Shtabovenko, R. Mertig and F. Orellana, FeynCalc 9.3: New features and improvements, Comput. Phys. Commun. 256 (2020) 107478 [arXiv:2001.04407] [INSPIRE].